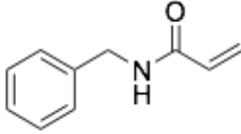
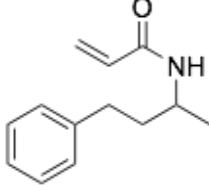
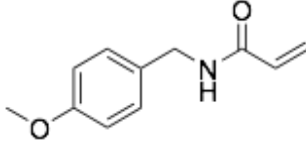
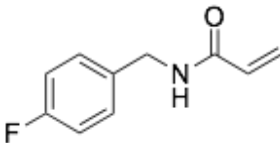
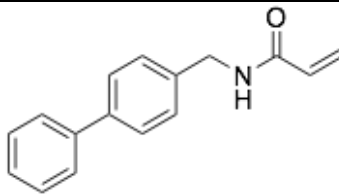
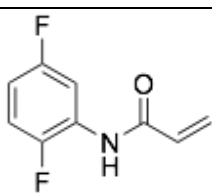
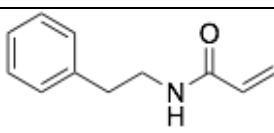
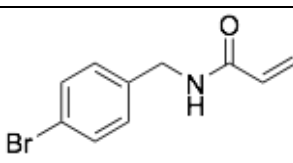
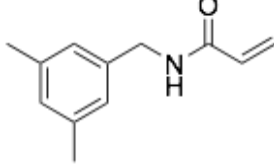


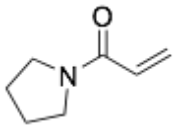
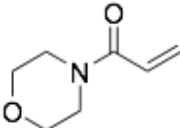
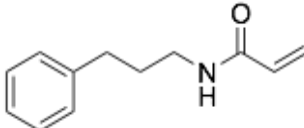
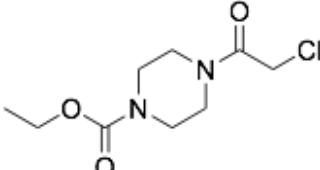
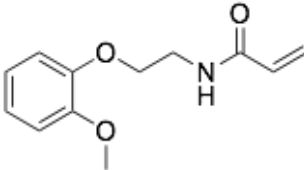
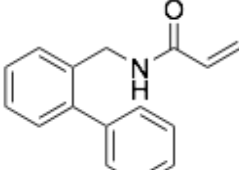
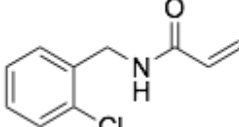
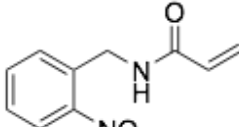
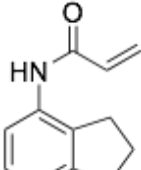
Supplementary Information

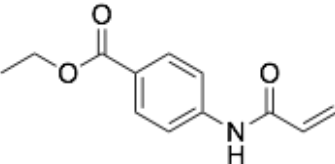
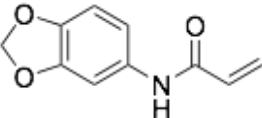
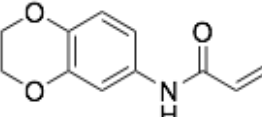
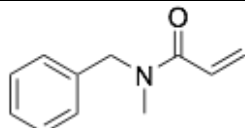
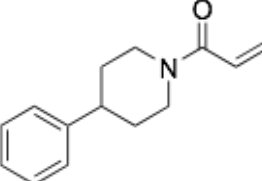
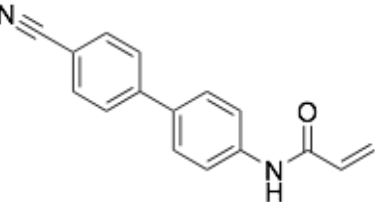
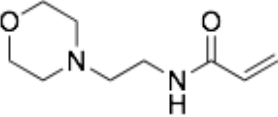
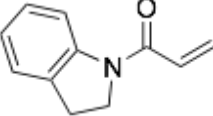
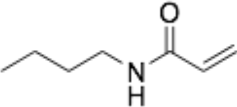
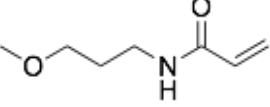
Supplementary Table 1. Small molecule screening data

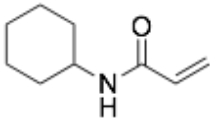
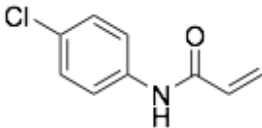
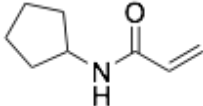
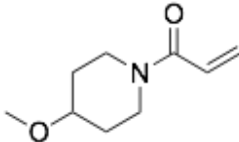
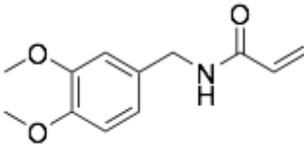
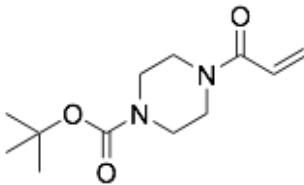
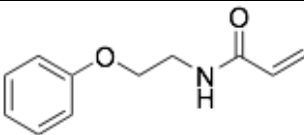
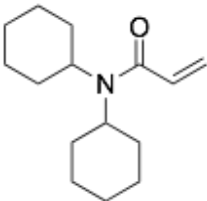
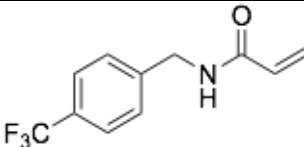
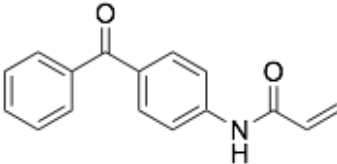
Category	Parameter	Description
Assay	Type of assay	Autophagy activation screen using a dual color fluorescent autophagic flux probe
	Target	Target not known
	Primary measurement	Degradation of LC3 by measuring GFP/RFP ratios
	Key reagents	a fluorescent probe GFP-LC3-RFP-LC3ΔG to measure autophagic flux
	Assay protocol	MEF cells stably expressing GFP-LC3-RFP-LC3ΔG were plated on 96-well plates (Corning; 3904) at 30,000 cells/well and allowed to grow in complete medium overnight. The cells were then incubated with covalent ligands (50 μM or at indicated concentrations), rapamycin (100 nM), Torin 1 (250 nM) or DMSO solvent control in complete medium (100 μL) for 24 h. After that, the medium was aspirated and the cells were fixed with 4% paraformaldehyde in PBS (100 μL) for 10 min, washed with PBS (100 μL) and assayed in PBS (100 μL) by SpectraMax i3 (Molecular Devices). GFP fluorescence was measured with excitation and emission at 488±9 nm and 514±15 nm respectively, while RFP fluorescence was measured with excitation and emission at 584±9 nm and 612±15 nm respectively.
	Additional comments	none
Library	Library size	217
	Library composition	Cysteine-reactive acrylamides and chloroacetamides; lysine-reactive dichlorotriazines
	Source	Previously synthesized in the Nomura Research Group and purchased from Enamine
	Additional comments	none
Screen	Format	96-well format
	Concentration(s) tested	50 μM
	Plate controls	DMSO vehicle-treated controls
	Reagent/ compound dispensing system	Standard pipetting
	Detection instrument and software	SpectraMax i3 (Molecular Devices)
	Assay validation/QC	Positive control mTORC1 inhibitors rapamycin and Torin1 were tested
	Correction factors	none
	Normalization	GFP levels were normalized to RFP levels
	Additional comments	none
Post-HTS analysis	Hit criteria	GFP/RFP ratios less than 0.8
	Hit rate	13 %
	Additional assay(s)	Additional screen in human HEK293A cells expression same autophagic flux probe to identify hits showed similar activity gave one primary hit EN6 (final hit rate 0.4 %)
	Confirmation of hit purity and structure	We resynthesized EN6 with >97 % purity and reconfirmed activity.
	Additional comments	none

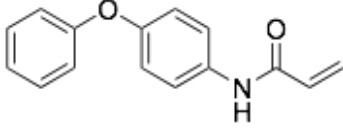
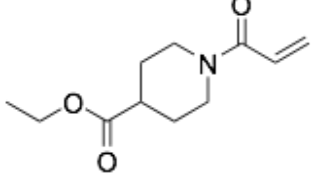
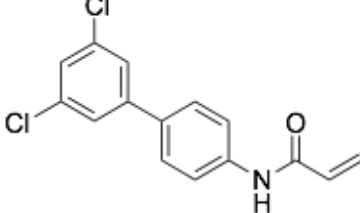
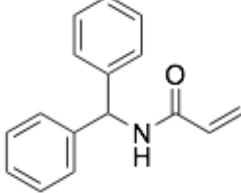
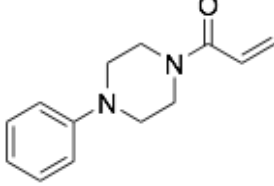
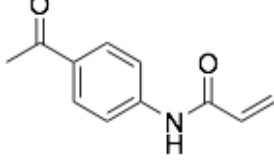
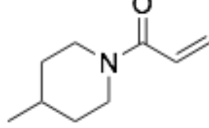
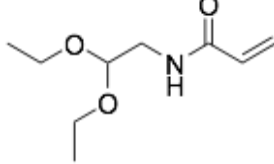
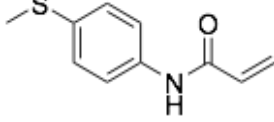
Supplementary Table 2. Cysteine-reactive acrylamide and chloroacetamide libraries

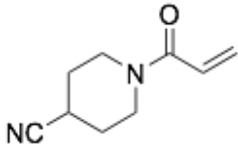
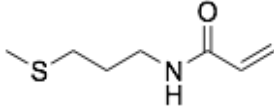
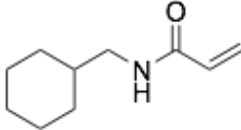
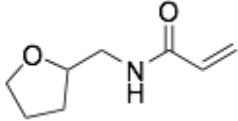
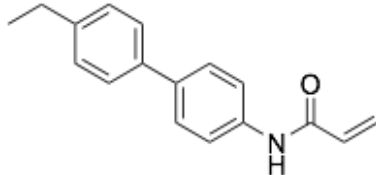
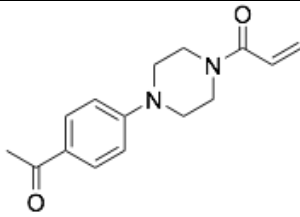
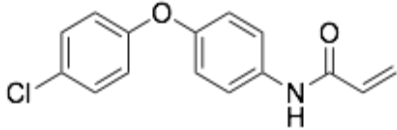
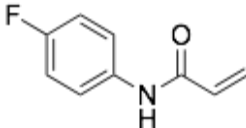
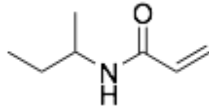
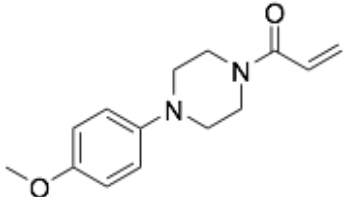
Compound	Compound Structure
DKM 2-31	 <chem>C=CC(=O)NCc1ccccc1</chem>
DKM 2-32	 <chem>C=CC(=O)NCCc1ccccc1</chem>
DKM 2-33	 <chem>C=CC(=O)NCc1ccc(OC)cc1</chem>
DKM 2-34	 <chem>C=CC(=O)NCc1ccc(F)cc1</chem>
DKM 2-37	 <chem>C=CC(=O)NCc1ccc(cc1)-c2ccccc2</chem>
DKM 2-40	 <chem>C=CC(=O)Nc1cc(F)c(F)cc1</chem>
DKM 2-42	 <chem>C=CC(=O)NCCc1ccccc1</chem>
DKM 2-43	 <chem>C=CC(=O)NCc1ccc(Br)cc1</chem>
DKM 2-47	 <chem>C=CC(=O)NCc1cc(C)c(C)cc1</chem>

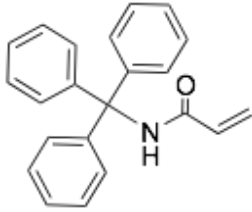
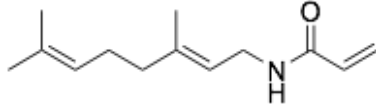
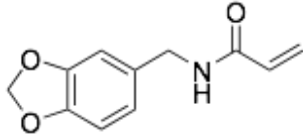
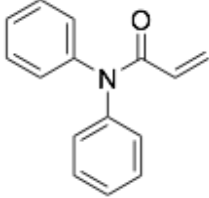
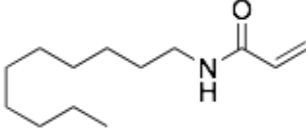
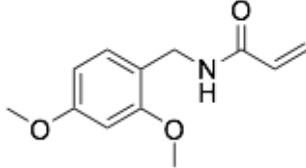
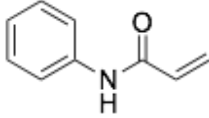
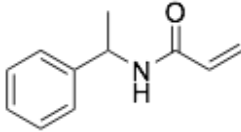
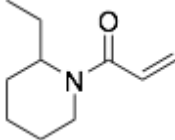
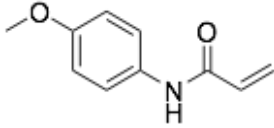
DKM 2-48	
DKM 2-49	
DKM 2-50	
DKM 2-52	
DKM 2-58	
DKM 2-59	
DKM 2-60	
DKM 2-62	
DKM 2-84	

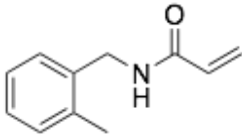
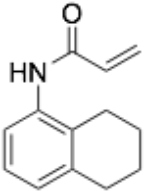
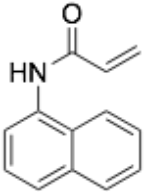
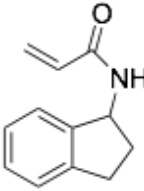
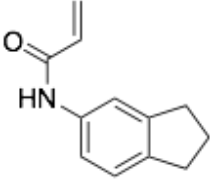
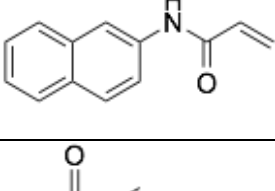
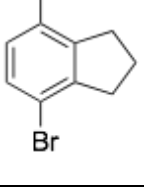
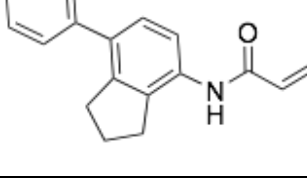
DKM 2-85	
DKM 2-86	
DKM 2-87	
DKM 2-95	 <p>(Two rotamers in equal amounts)</p>
DKM 2-97	
DKM 2-98	
DKM 2-100	
DKM 2-101	
DKM 2-102	
DKM 2-103	

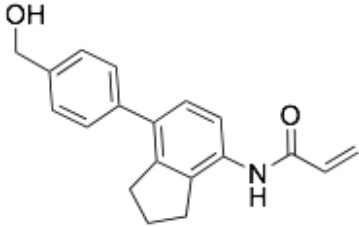
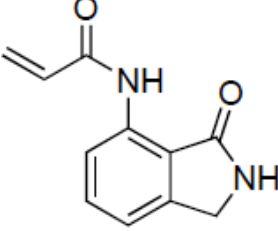
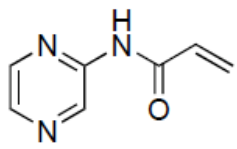
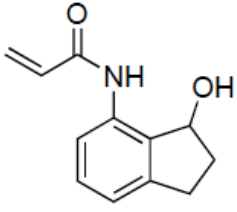
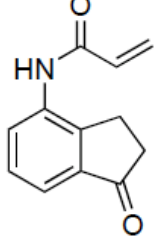
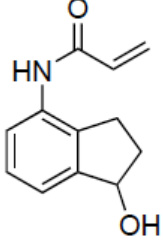
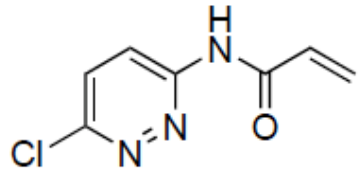
DKM 2-106	
DKM 2-107	
DKM 2-108	
DKM 2-109	
DKM 2-110	
DKM 2-111	
DKM 2-113	
DKM 2-114	
DKM 2-116	
DKM 2-117	

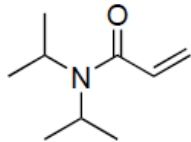
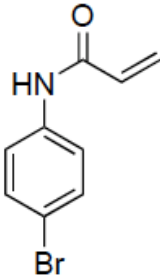
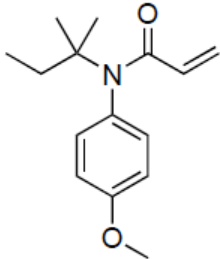
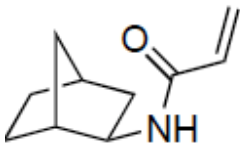
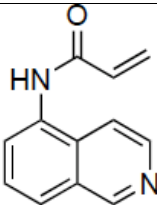
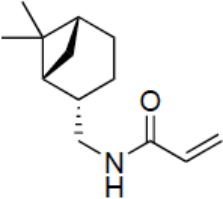
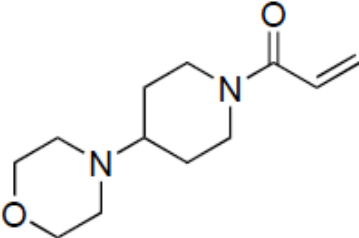
DKM 2-119	 <chem>C=CC(=O)Nc1ccc(Oc2ccccc2)cc1</chem>
DKM 2-120	 <chem>C=CC(=O)NCC(=O)OCC</chem>
DKM 3-3	 <chem>C=CC(=O)Nc1ccc(cc1)-c2cc(Cl)cc(Cl)c2</chem>
DKM 3-4	 <chem>C=CC(=O)Nc1ccc(cc1)C2=CC=CC=C2C3=CC=CC=C3</chem>
DKM 3-5	 <chem>C=CC(=O)NCCNc1ccccc1</chem>
DKM 3-7	 <chem>C=CC(=O)Nc1ccc(C(=O)C)cc1</chem>
DKM 3-8	 <chem>C=CC(=O)N1CCN(CC1)C</chem>
DKM 3-9	 <chem>C=CC(=O)NCC(=O)OCCOCC</chem>
DKM 3-10	 <chem>C=CC(=O)Nc1ccc(C)cc1</chem>

DKM 3-11	 <chem>NC(=O)C=Cc1ccc(C#N)cc1</chem>
DKM 3-12	 <chem>CC(C)CCNC(=O)C=C</chem>
DKM 3-13	 <chem>C1CCCCC1CN(C=O)C=C</chem>
DKM 3-15	 <chem>C1CCOC1CN(C=O)C=C</chem>
DKM 3-16	 <chem>CCc1ccc(NC(=O)C=C)cc1</chem>
DKM 3-29	 <chem>CC(=O)c1ccc(NC(=O)C=C)cc1</chem>
DKM 3-30	 <chem>Clc1ccc(NC(=O)C=C)cc1</chem>
DKM 3-31	 <chem>Fc1ccc(NC(=O)C=C)cc1</chem>
DKM 3-32	 <chem>CC(C)CCNC(=O)C=C</chem>
DKM 3-36	 <chem>COC1=CC=C(NC(=O)C=C)C=C1</chem>

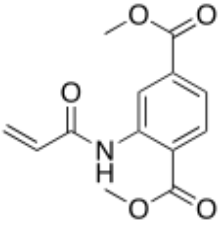
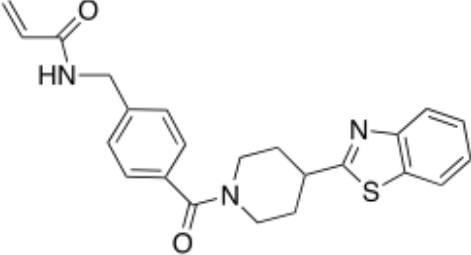
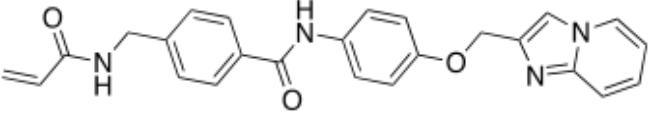
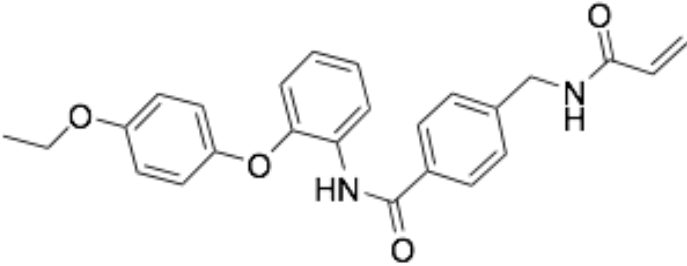
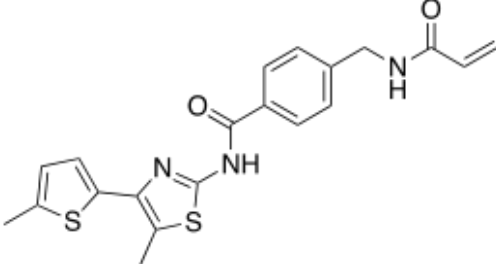
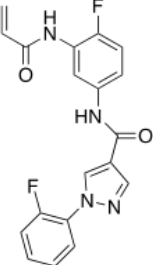
DKM 3-41	
DKM 3-42	
DKM 3-43	
DKM 3-70	
TRH 1-12	
TRH 1-13	
TRH 1-19	
TRH 1-20	
TRH 1-27	
TRH 1-32	

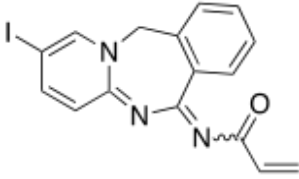
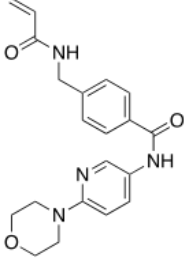
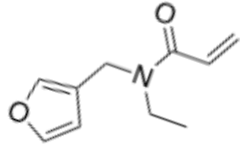
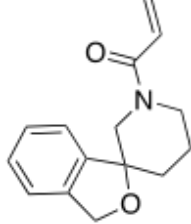
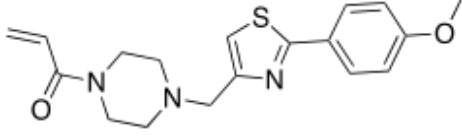
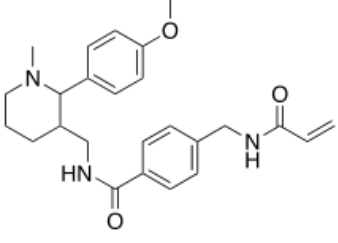
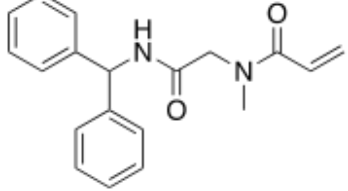
TRH 1-54	 <chem>CC1=CC=C(C=C1)NC(=O)C=C</chem>
TRH 1-56	 <chem>C1=CC=C2CCCCC2C1NC(=O)C=C</chem>
TRH 1-57	 <chem>C1=CC=C2C=CC3=CC=CC=C3C2=C1NC(=O)C=C</chem>
TRH 1-58	 <chem>C1=CC=C2C=CC1C2NC(=O)C=C</chem>
TRH 1-59	 <chem>C1=CC=C2C=CC1C2NC(=O)C=C</chem>
TRH 1-60	 <chem>C1=CC=C2C=CC1C2NC(=O)C=C</chem>
TRH 1-65	 <chem>C1=CC=C2C=CC1C2NC(=O)C=C</chem>
TRH 1-68	 <chem>C1=CC=C2C=CC1C2NC(=O)C=C</chem>

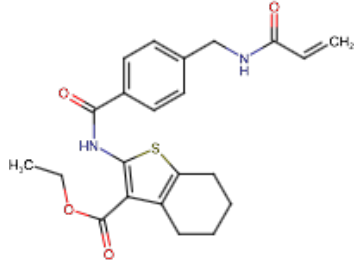
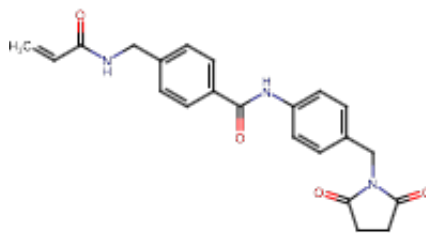
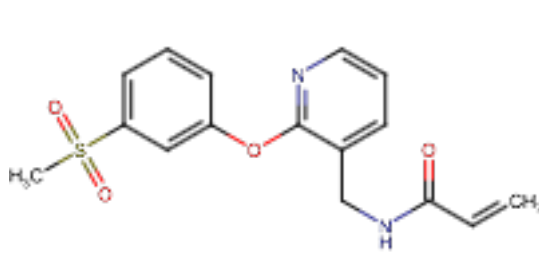
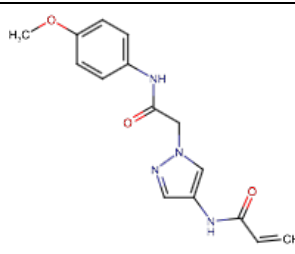
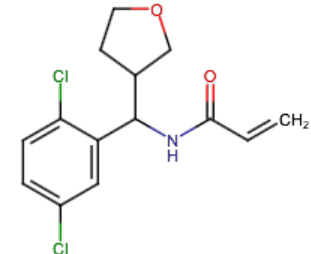
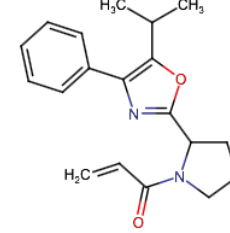
TRH 1-70	
TRH 1-152	
TRH 1-156	
TRH 1-133	
TRH 1-134	
TRH 1-135	
TRH 1-155	

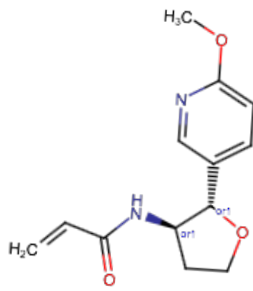
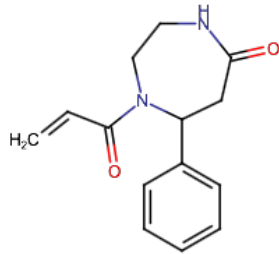
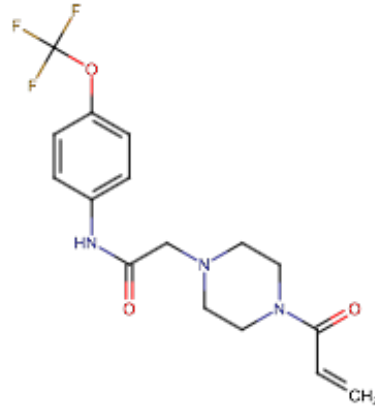
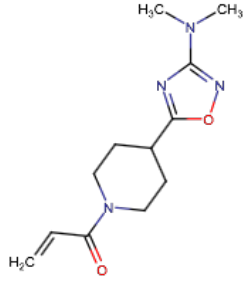
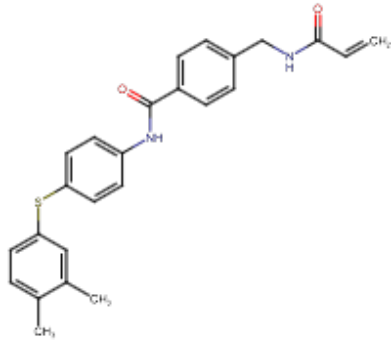
TRH 1-167	
YP 1-36	
TRH 1-170	
TRH 1-176	 <p>(racemic)</p>
TRH 1-162	
TRH 1-178	
YP 1-42	

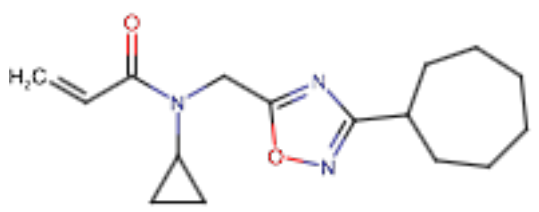
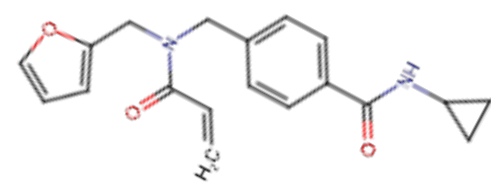
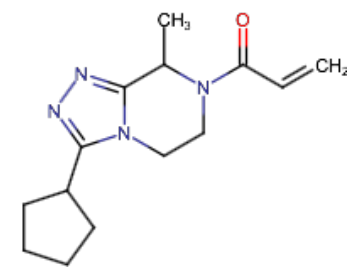
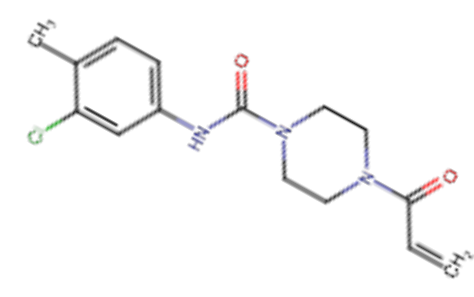
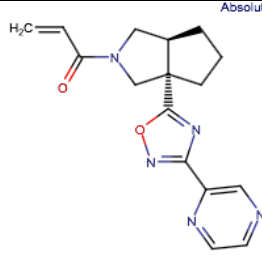
Supplementary Table 3. Cysteine-reactive acrylamide and chloroacetamide libraries from Enamine

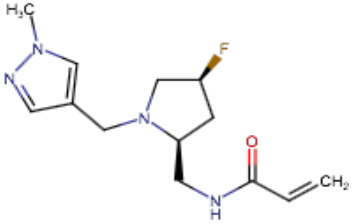
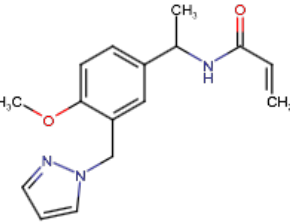
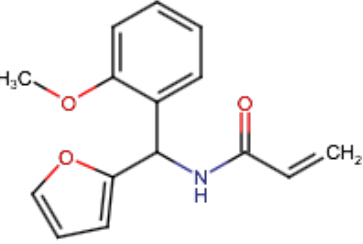
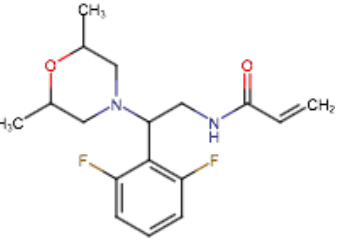
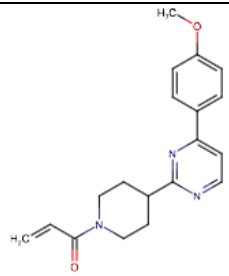
Compound	Compound Structure
EN1	
EN2	
EN3	
EN4	
EN5	
EN6	

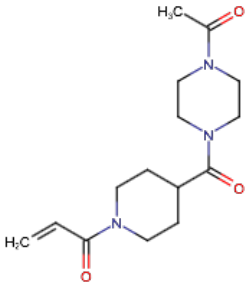
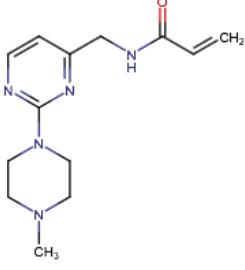
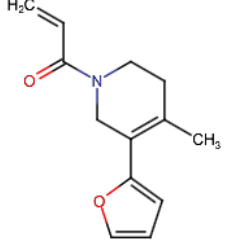
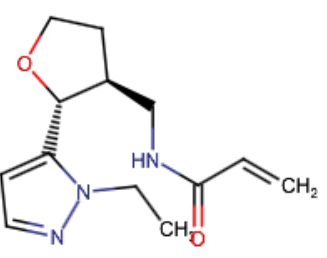
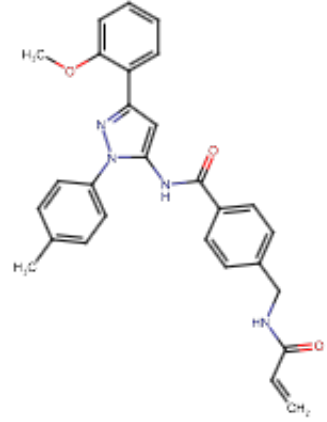
EN7	
EN8	
EN9	
EN10	
EN12	
EN13	
EN14	

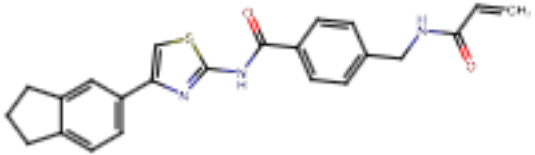
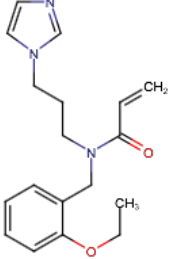
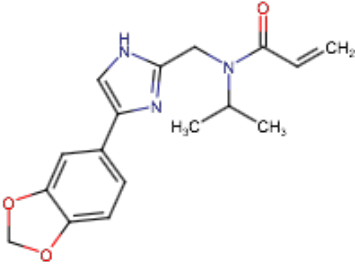
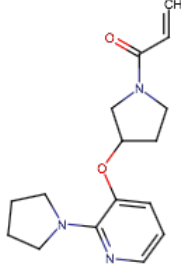
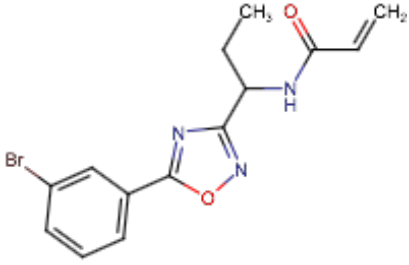
EN15	 <p>Chemical structure of a complex molecule featuring a benzothiazine core, a methoxy group, and a 2-acrylamidoethyl side chain.</p>
EN16	 <p>Chemical structure of a molecule with a central benzene ring, a methoxy group, and a 2-acrylamidoethyl side chain.</p>
EN17	 <p>Chemical structure of a molecule with a central benzene ring, a methoxy group, and a 2-acrylamidoethyl side chain.</p>
EN18	 <p>Chemical structure of a molecule with a central benzene ring, a methoxy group, and a 2-acrylamidoethyl side chain.</p>
EN19	 <p>Chemical structure of a molecule with a central benzene ring, a methoxy group, and a 2-acrylamidoethyl side chain.</p>
EN20	 <p>Chemical structure of a molecule with a central benzene ring, a methoxy group, and a 2-acrylamidoethyl side chain.</p>

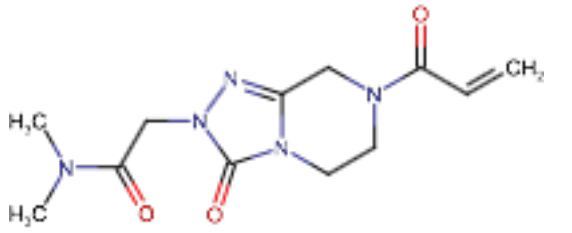
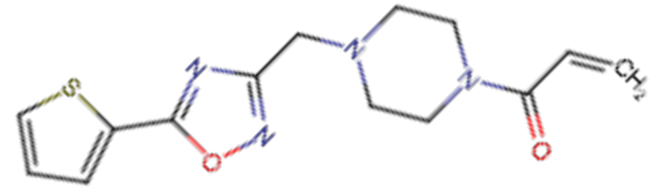
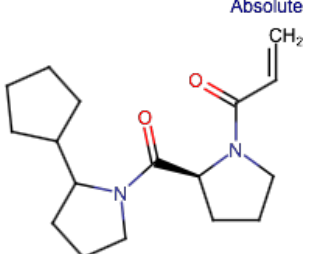
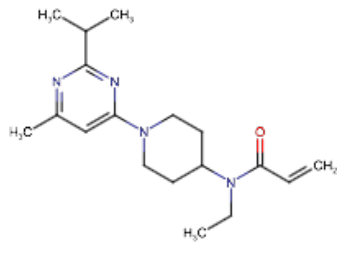
EN21	 <p>Chemical structure of a chiral molecule. It features a morpholine ring with a methoxy group (-OCH₃) at the 4-position. The morpholine ring is substituted at the 2-position with an acrylamide group (-NH-C(=O)-CH=CH₂). The stereochemistry is indicated with a wedge bond to the nitrogen and a dashed bond to the oxygen.</p>
EN22	 <p>Chemical structure of a piperazine ring substituted with a benzene ring and an acrylamide group (-NH-C(=O)-CH=CH₂).</p>
EN23	 <p>Chemical structure of a piperazine ring substituted with a trifluoromethoxy group (-OCF₃), an acrylamide group (-NH-C(=O)-CH=CH₂), and a propyl chain (-CH₂-CH₂-CH₂-) connecting the two nitrogen atoms.</p>
EN24	 <p>Chemical structure of a piperazine ring substituted with a dimethylamino group (-N(CH₃)₂), an oxadiazole ring, and an acrylamide group (-NH-C(=O)-CH=CH₂).</p>
EN25	 <p>Chemical structure of a complex molecule. It features a thioether group (-S-) connecting two benzene rings. One benzene ring is substituted with a methyl group (-CH₃). The other benzene ring is substituted with an acrylamide group (-NH-C(=O)-CH=CH₂).</p>

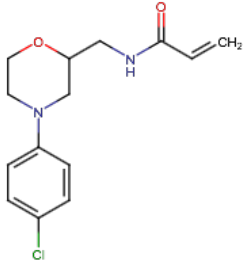
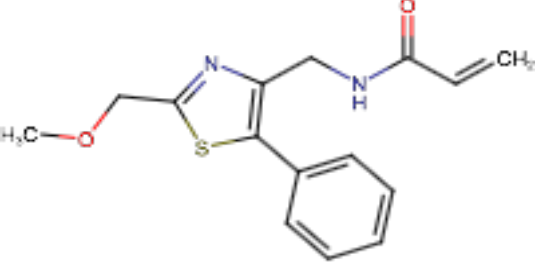
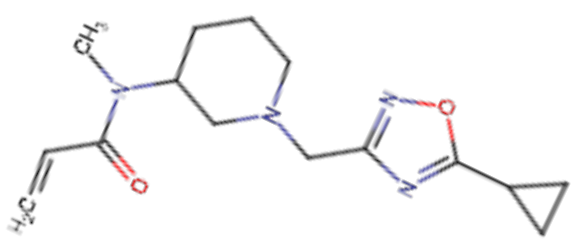
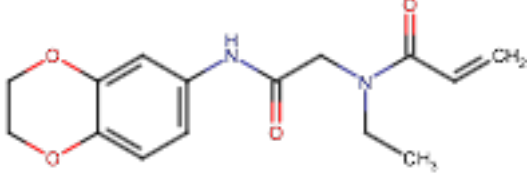
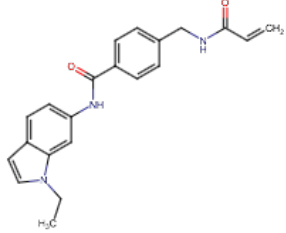
<p>EN26</p>	 <p>Chemical structure of a molecule featuring a vinyl group ($\text{H}_2\text{C}=\text{CH}-$), a cyclopropyl ring, a 1,3,4-oxadiazole ring, and a cyclooctane ring.</p>
<p>EN27</p>	 <p>Chemical structure of a molecule featuring a furfuryl group, a vinyl group ($\text{H}_2\text{C}=\text{CH}-$), a benzene ring, and a cyclopropyl ring.</p>
<p>EN28</p>	 <p>Chemical structure of a molecule featuring a methyl group (CH_3), a vinyl group ($\text{CH}_2=\text{CH}-$), a bicyclic nitrogen-containing ring system, and a cyclopentane ring.</p>
<p>EN29</p>	 <p>Chemical structure of a molecule featuring a chloromethyl group (CH_2Cl), a methyl group (CH_3), a piperazine ring, and a vinyl group ($\text{CH}_2=\text{CH}-$).</p>
<p>EN30</p>	<p>Absolute</p>  <p>Chemical structure of a molecule featuring a vinyl group ($\text{H}_2\text{C}=\text{CH}-$), a bicyclic nitrogen-containing ring system, a 1,3,4-oxadiazole ring, and a pyridine ring.</p>

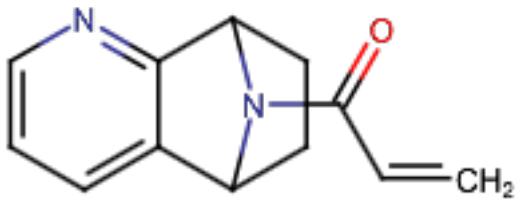
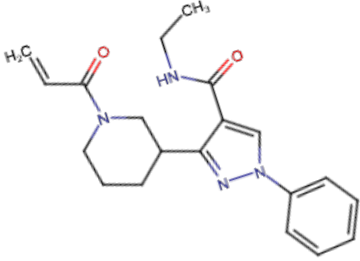
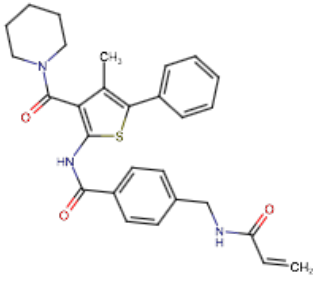
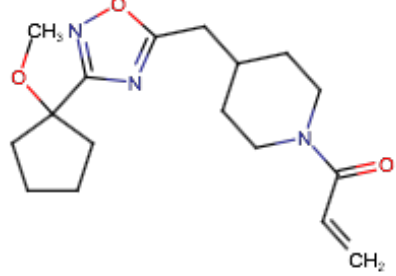
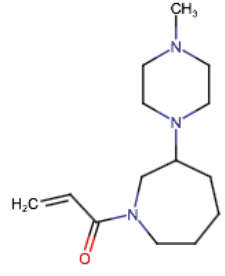
<p>EN32</p>	<p>Absolute</p> 
<p>EN33</p>	
<p>EN35</p>	
<p>EN36</p>	
<p>EN37</p>	

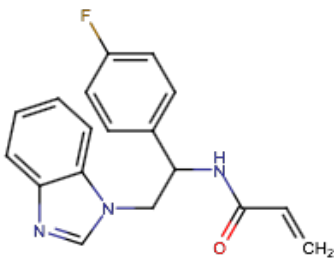
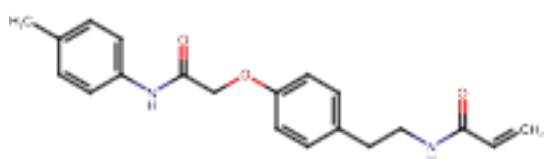
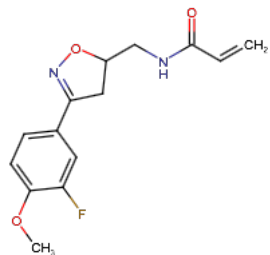
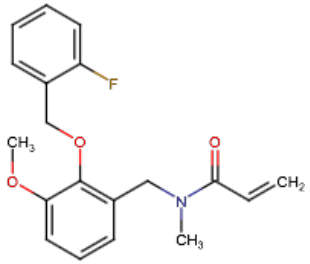
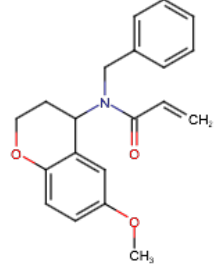
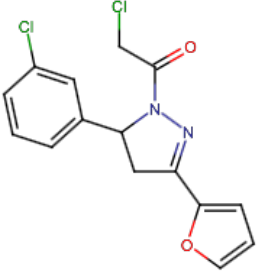
<p>EN38</p>	
<p>EN39</p>	
<p>EN40</p>	
<p>EN43</p>	
<p>EN44</p>	

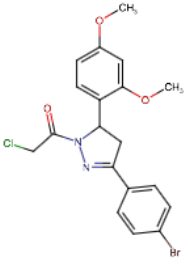
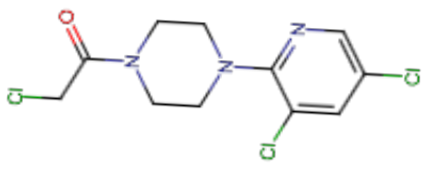
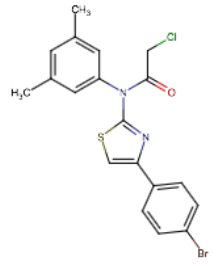
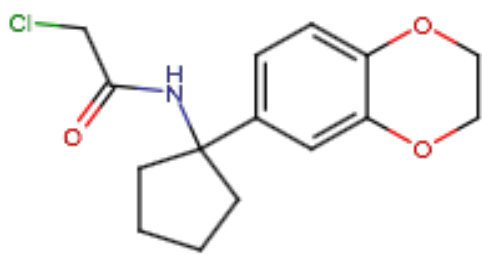
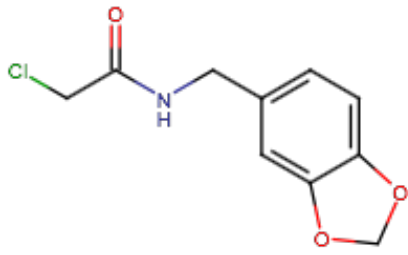
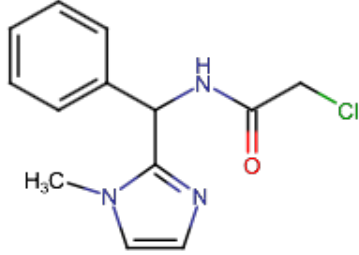
<p>EN45</p>	
<p>EN46</p>	
<p>EN47</p>	
<p>EN48</p>	
<p>EN49</p>	

<p>EN50</p>	
<p>EN51</p>	
<p>EN52</p>	
<p>EN53</p>	

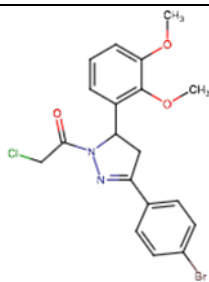
<p>EN54</p>	
<p>EN55</p>	
<p>EN57</p>	
<p>EN58</p>	
<p>EN59</p>	

EN60	
EN61	
EN62	
EN63	
EN64	

EN65	
EN66	
EN67	
EN68	
EN69	
EN70	

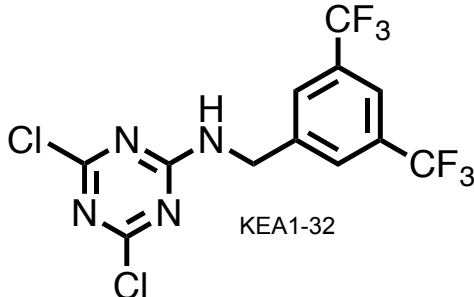
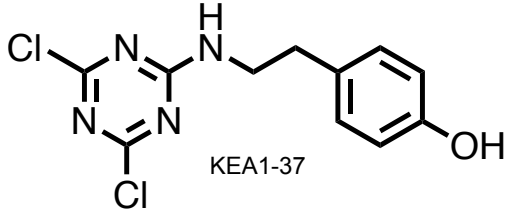
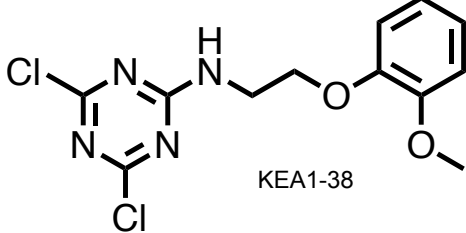
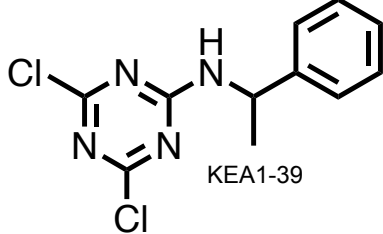
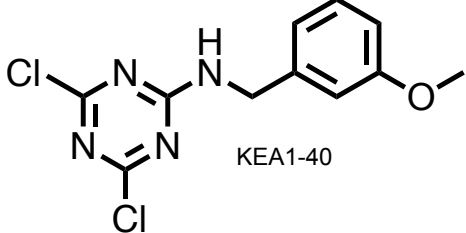
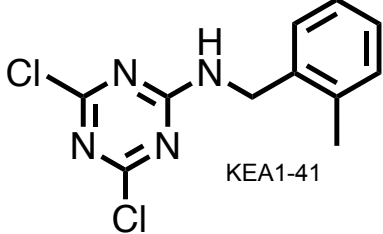
EN71	
EN75	
EN80	
EN84	
EN85	
EN86	

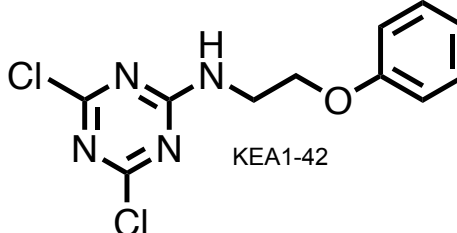
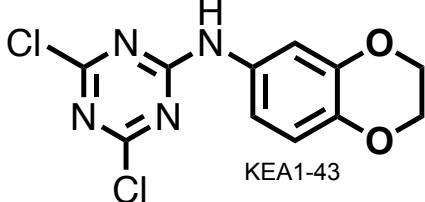
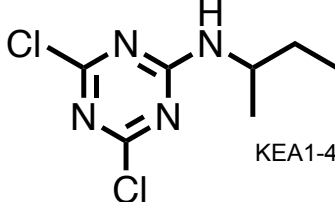
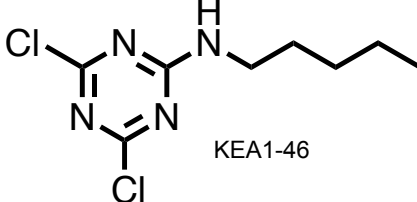
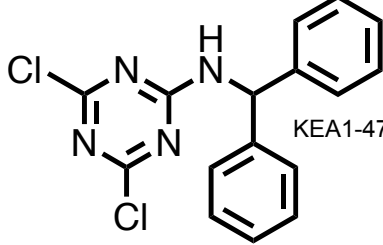
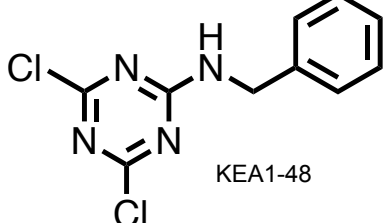
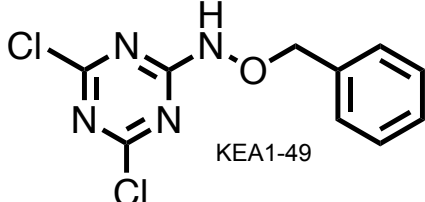
EN103

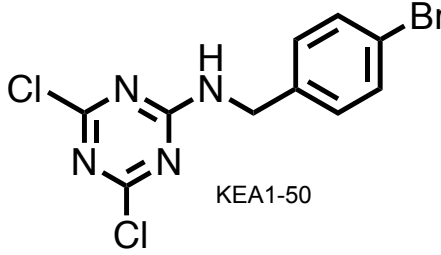
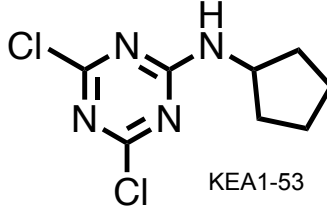
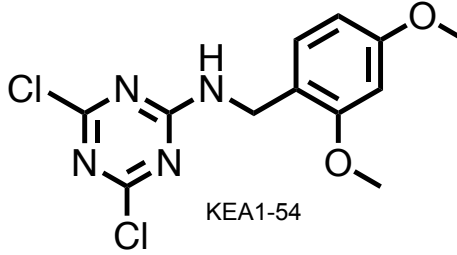
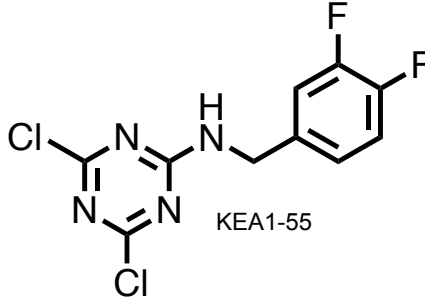
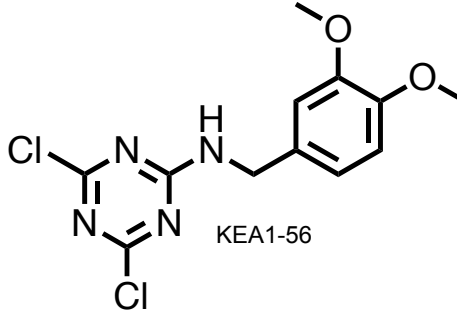
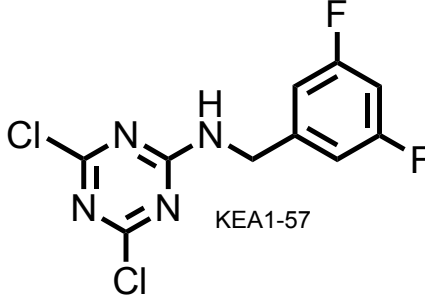


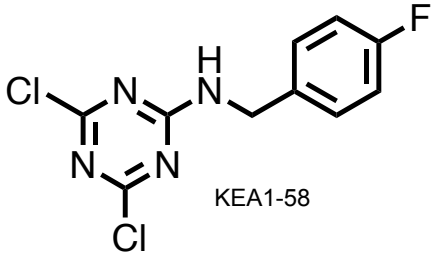
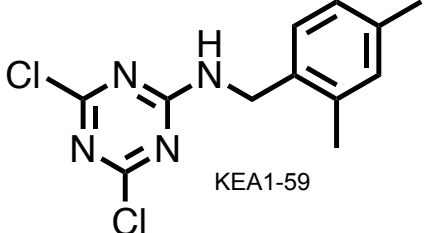
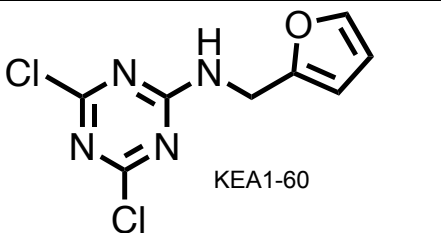
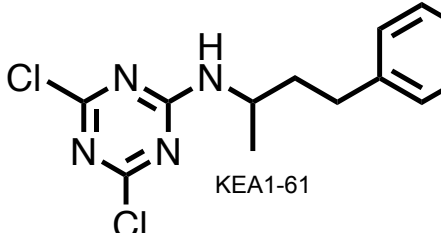
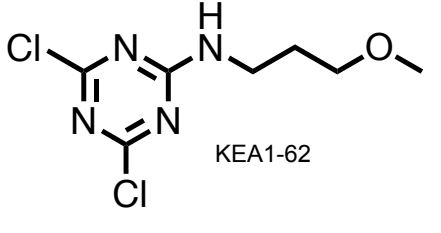
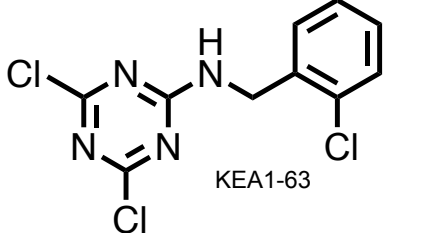
Supplementary Table 4. Dichlorotriazine libraries

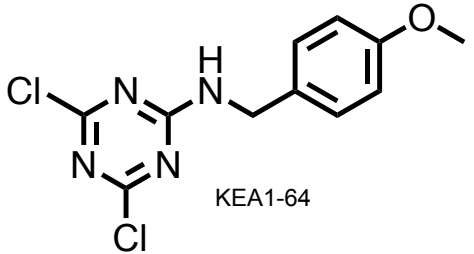
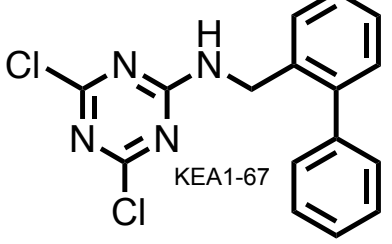
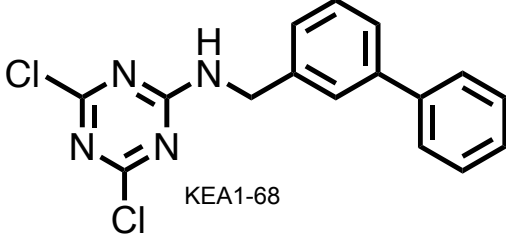
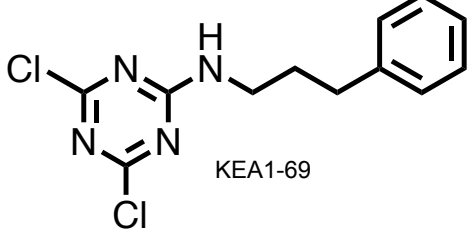
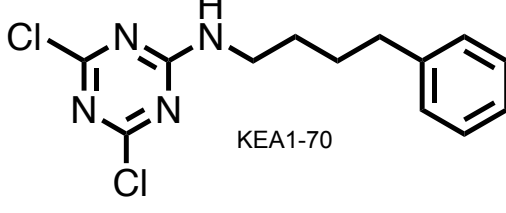
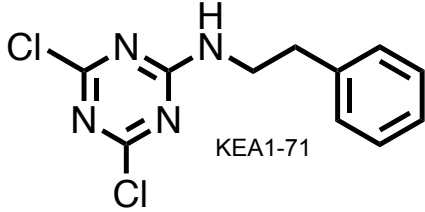
Compound	Compound Structure
KEA 1-22	 KEA1-22
KEA 1-23	 KEA1-23
KEA 1-30	 KEA1-30
KEA 1-31	 KEA1-31

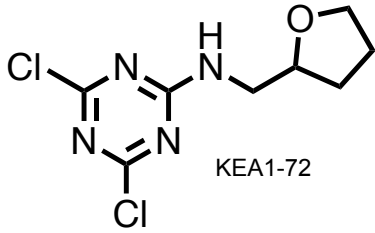
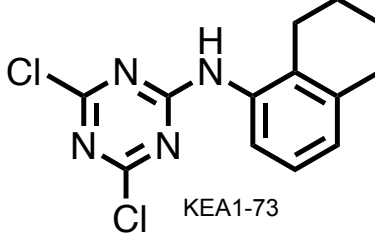
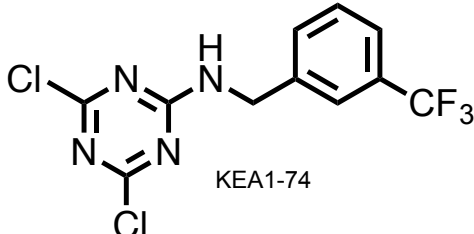
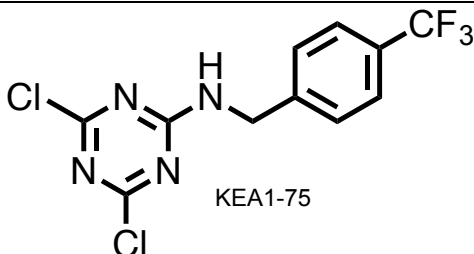
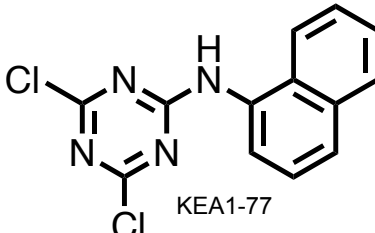
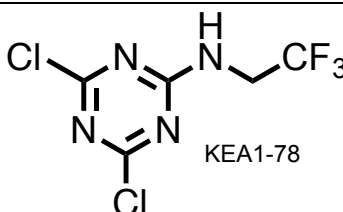
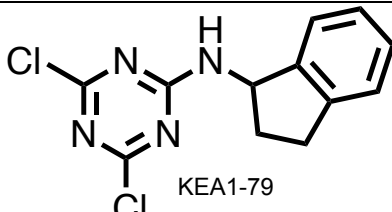
<p>KEA 1-32</p>	 <p>KEA1-32</p>
<p>KEA 1-37</p>	 <p>KEA1-37</p>
<p>KEA 1-38</p>	 <p>KEA1-38</p>
<p>KEA 1-39</p>	 <p>KEA1-39</p>
<p>KEA 1-40</p>	 <p>KEA1-40</p>
<p>KEA 1-41</p>	 <p>KEA1-41</p>

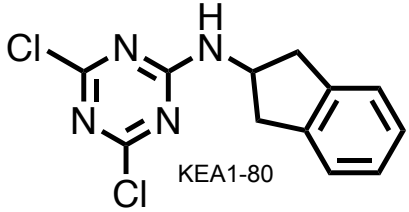
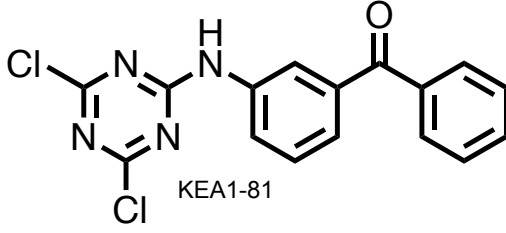
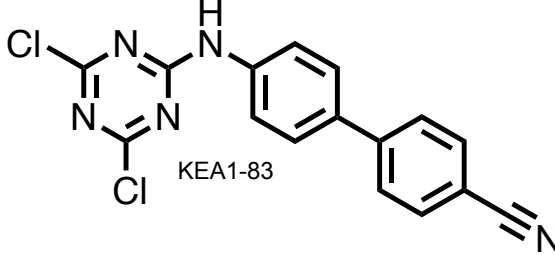
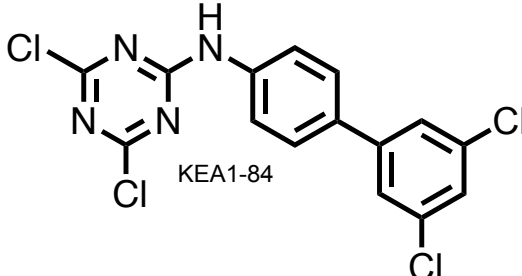
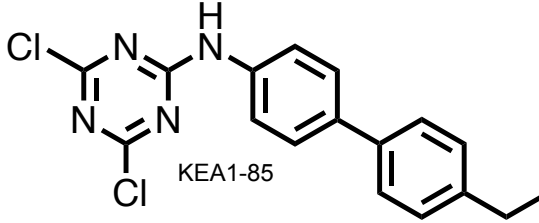
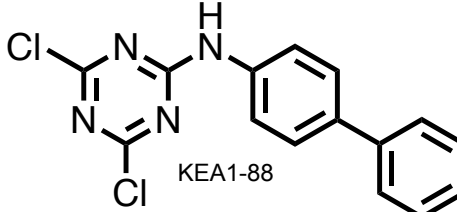
KEA 1-42	 KEA1-42
KEA 1-43	 KEA1-43
KEA 1-45	 KEA1-45
KEA 1-46	 KEA1-46
KEA 1-47	 KEA1-47
KEA 1-48	 KEA1-48
KEA 1-49	 KEA1-49

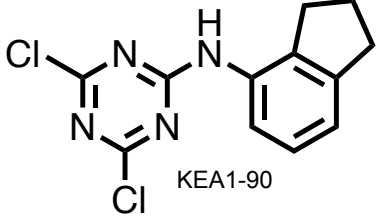
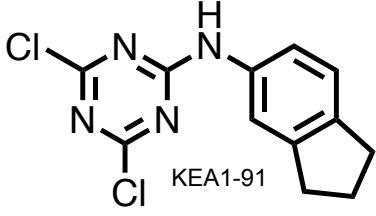
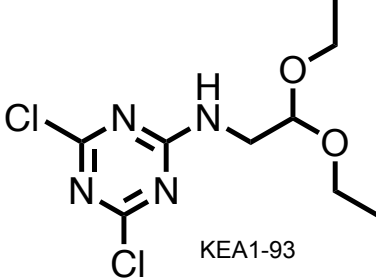
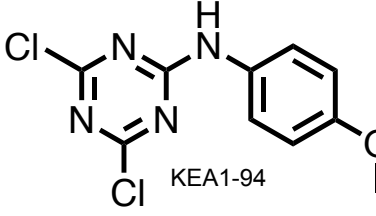
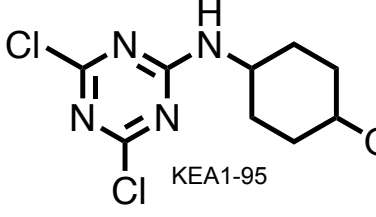
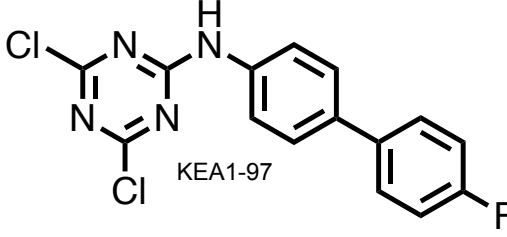
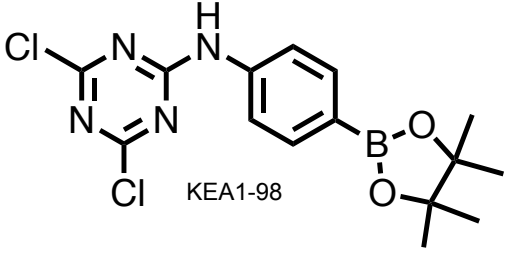
KEA 1-50	 <p>KEA1-50</p>
KEA 1-53	 <p>KEA1-53</p>
KEA 1-54	 <p>KEA1-54</p>
KEA 1-55	 <p>KEA1-55</p>
KEA 1-56	 <p>KEA1-56</p>
KEA 1-57	 <p>KEA1-57</p>

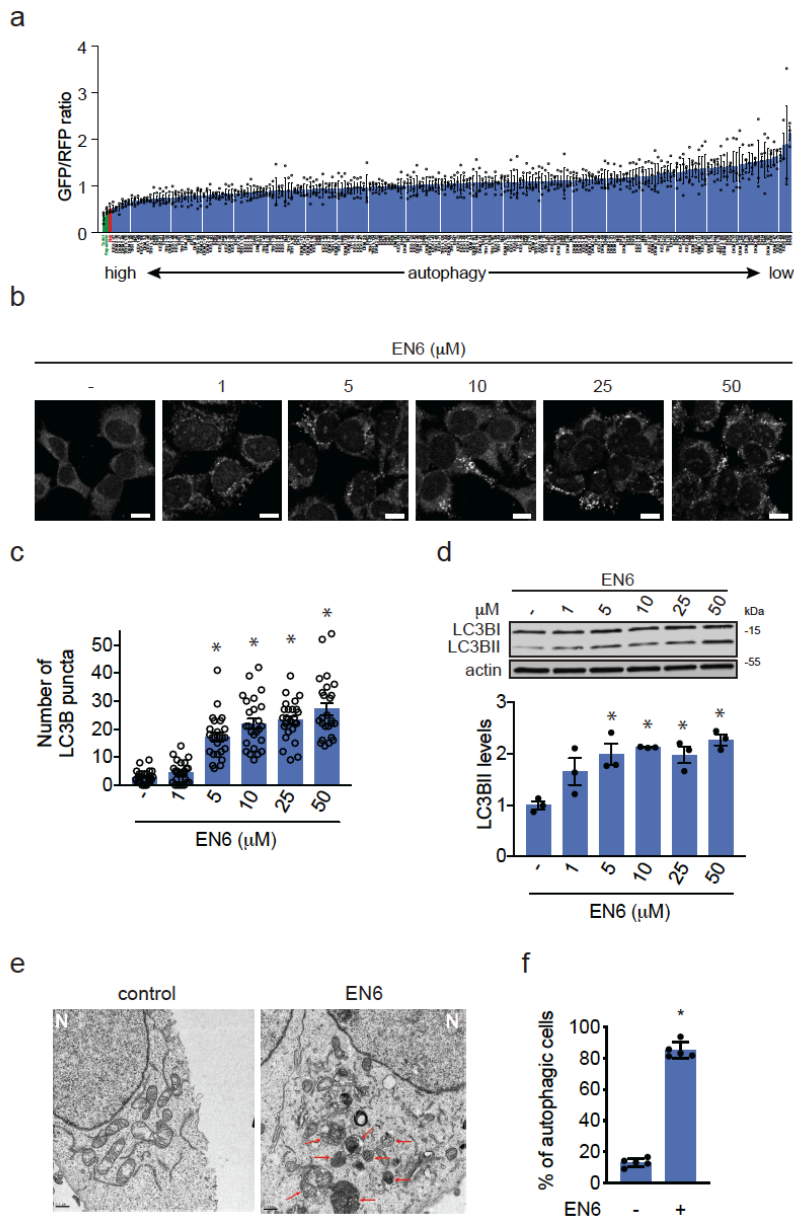
<p>KEA 1-58</p>	 <p>KEA1-58</p>
<p>KEA 1-59</p>	 <p>KEA1-59</p>
<p>KEA 1-60</p>	 <p>KEA1-60</p>
<p>KEA 1-61</p>	 <p>KEA1-61</p>
<p>KEA 1-62</p>	 <p>KEA1-62</p>
<p>KEA 1-63</p>	 <p>KEA1-63</p>

KEA 1-64	 <p>KEA1-64</p>
KEA 1-67	 <p>KEA1-67</p>
KEA 1-68	 <p>KEA1-68</p>
KEA 1-69	 <p>KEA1-69</p>
KEA 1-70	 <p>KEA1-70</p>
KEA 1-71	 <p>KEA1-71</p>

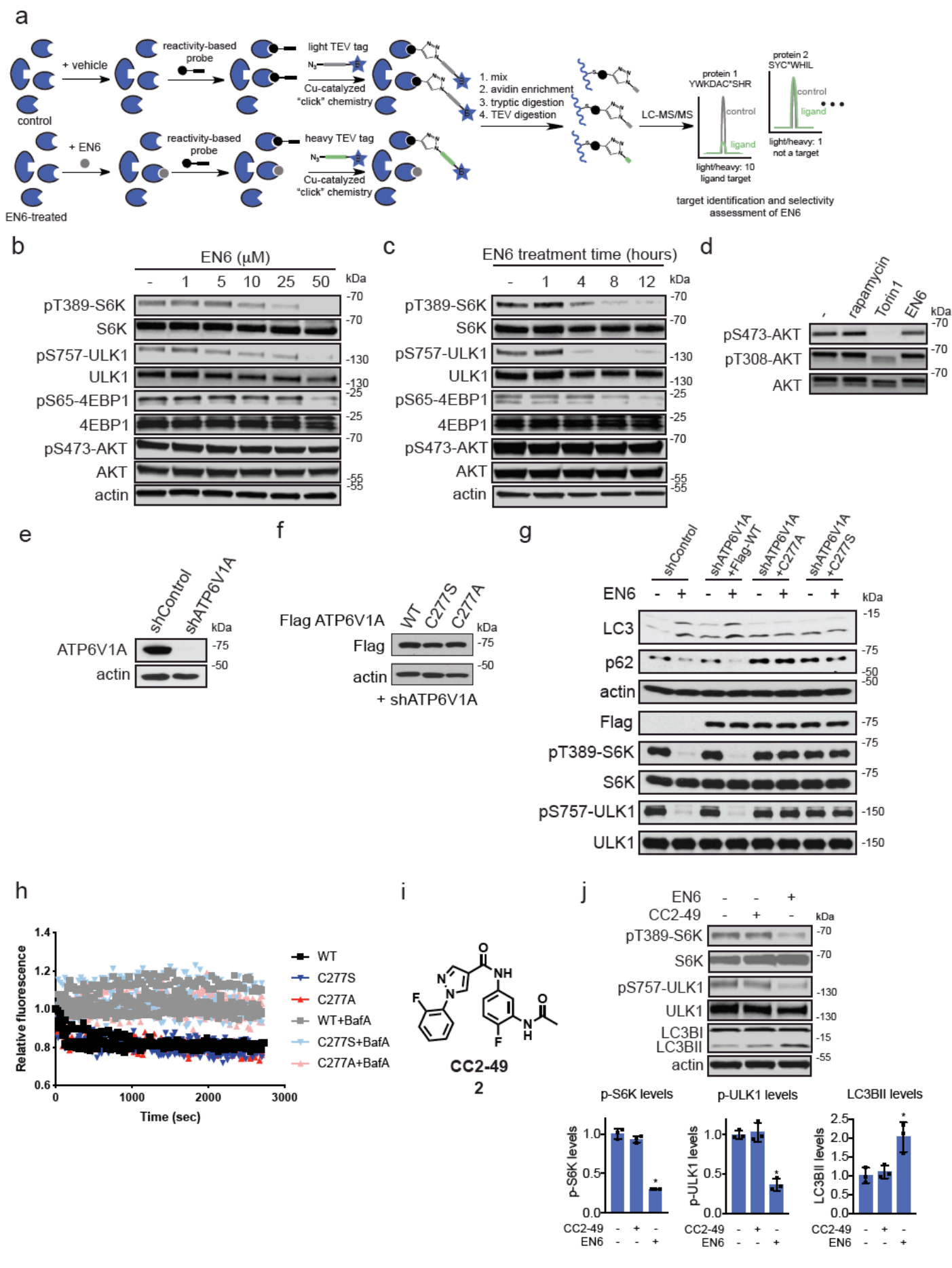
KEA 1-72	 <p>KEA1-72</p>
KEA 1-73	 <p>KEA1-73</p>
KEA 1-74	 <p>KEA1-74</p>
KEA 1-75	 <p>KEA1-75</p>
KEA 1-77	 <p>KEA1-77</p>
KEA 1-78	 <p>KEA1-78</p>
KEA 1-79	 <p>KEA1-79</p>

<p>KEA 1-80</p>	 <p>KEA1-80</p>
<p>KEA 1-81</p>	 <p>KEA1-81</p>
<p>KEA 1-83</p>	 <p>KEA1-83</p>
<p>KEA 1-84</p>	 <p>KEA1-84</p>
<p>KEA 1-85</p>	 <p>KEA1-85</p>
<p>KEA 1-88</p>	 <p>KEA1-88</p>

<p>KEA 1-90</p>	 <p>KEA1-90</p>
<p>KEA 1-91</p>	 <p>KEA1-91</p>
<p>KEA 1-93</p>	 <p>KEA1-93</p>
<p>KEA 1-94</p>	 <p>KEA1-94</p>
<p>KEA 1-95</p>	 <p>KEA1-95</p>
<p>KEA 1-97</p>	 <p>KEA1-97</p>
<p>KEA 1-98</p>	 <p>KEA1-98</p>

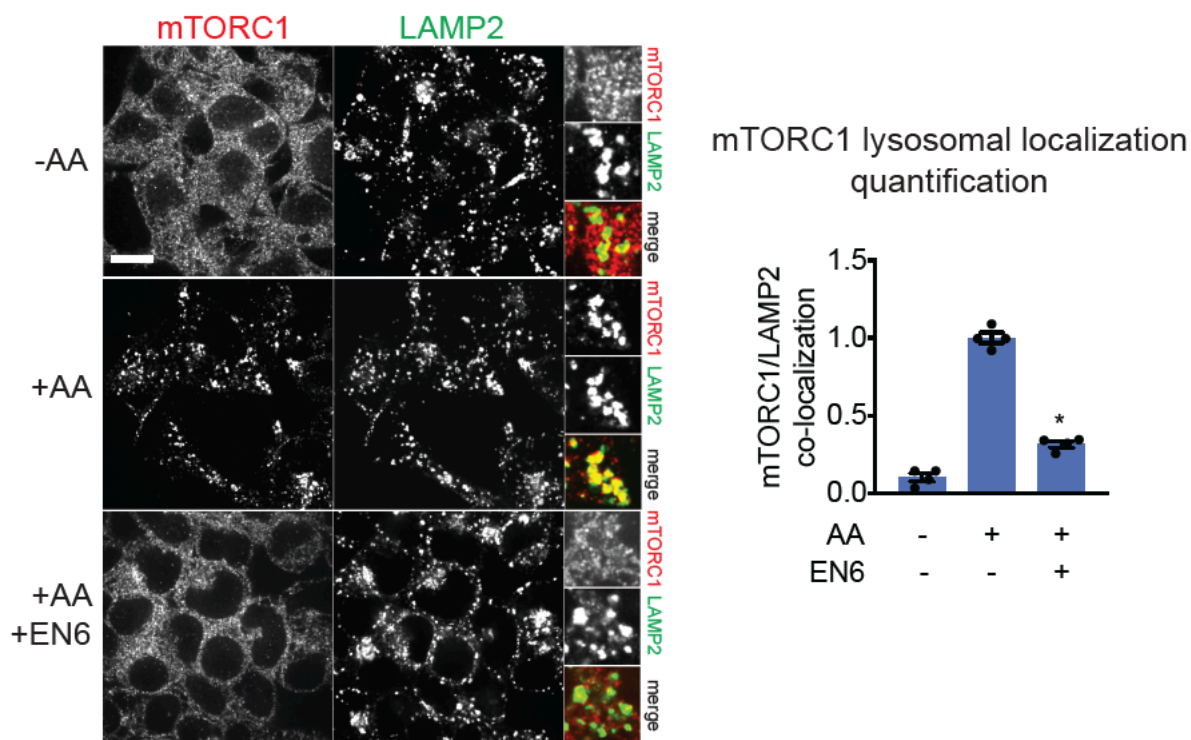


Supplementary Fig. 1. Dose-dependent activation of autophagy in HEK293A cells by EN6. (a) A covalent ligand screen in MEF cells. MEF cells expressing a fluorescent probe GFP-LC3-RFP-LC3ΔG to measure autophagic flux, were treated with vehicle DMSO or a covalent ligand (50 μM) for 24 h and GFP/RFP ratios were analyzed. Detailed data can be found in **Supplementary Dataset 1. (b)** Confocal fluorescence microscopy images and **(c)** Quantification of LC3B puncta in HEK293A cells treated by EN6 at indicated concentrations for 4 h. Scale bar in **(b)** denotes 10 μm. **(d)** Western blotting of LC3B level in HEK293A cells treated by EN6 at indicated concentrations for 4 h. Original gel images are in **Supplementary Fig. 12a. (e)** Representative transmission electron microscopy (TEM) images from HEK293A cells treated with DMSO vehicle control or EN6 (25 μM) for 4 h from n=5 biologically independent samples/group. Red arrows indicate autophagosomes and autolysosomes. “N” denotes the nucleus. Scale bar in **(e)** denotes 0.5 μm. **(f)** Percentage of cells that show autophagic structures from TEM analysis of HEK293A cells treated with DMSO vehicle DMSO control or EN6 (25 μM) for 4 h. Data shown in **(c, d, f)** are average ± sem, n=25 individual cells from 3 biologically independent samples/group for **(c)**, and n=3 for **(d)** and n=5 for **(f)** biologically independent samples/group. Statistical significance was calculated with unpaired two-tailed Student’s t-tests. Significance is expressed as *p=1.3x10⁻¹¹, 1.3x10⁻¹³, 4.7x10⁻¹⁸, and 1.6x10⁻¹⁴ for 5, 10, 25, and 50 μM, respectively, in **(c)** compared to vehicle-treated control groups; *p=1.2x10⁻⁴, 5.5x10⁻³, and 6.1x10⁻⁴ for 10, 25, and 50 μM, respectively, in **(d)** compared to vehicle-treated control groups; *p=3.1x10⁻⁹ for EN6-treated groups compared to vehicle-treated control groups.

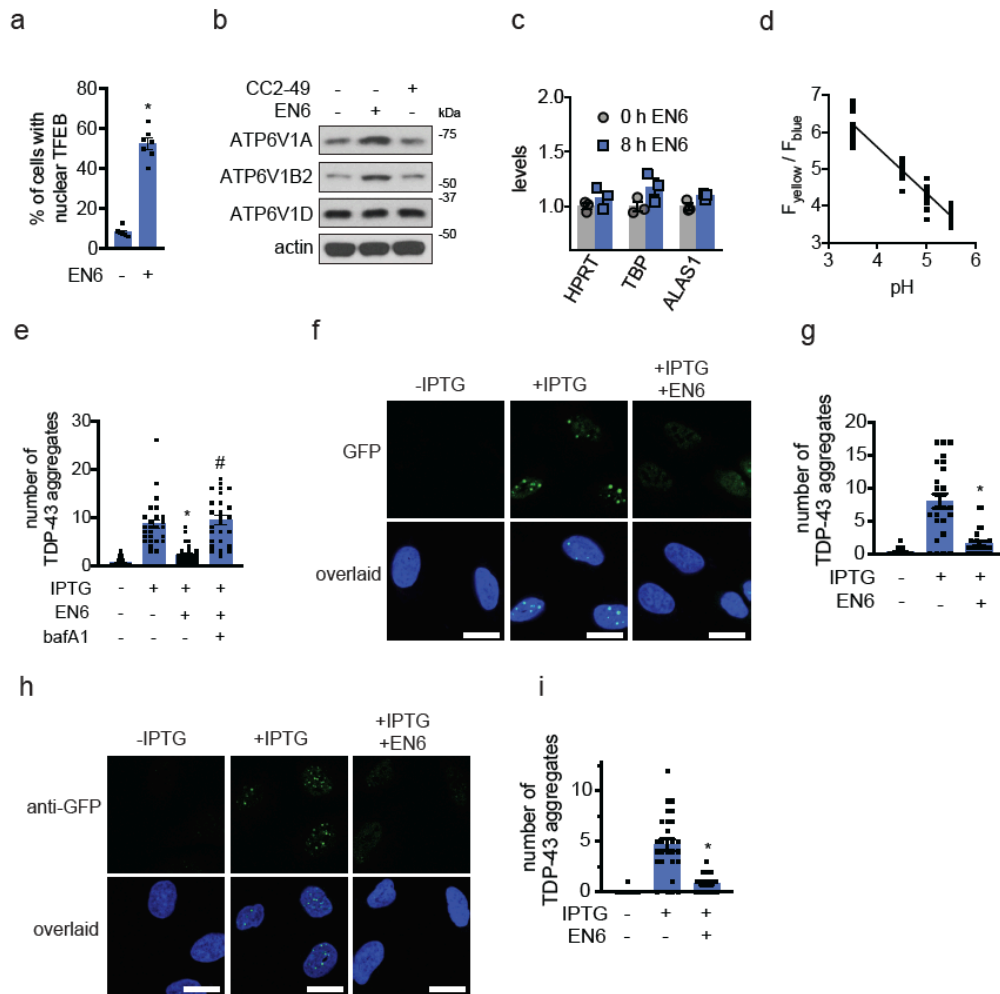


Supplementary Figure 2. Effect of EN6 and cysteine non-reactive EN6 analog CC2-49 on cell signaling.

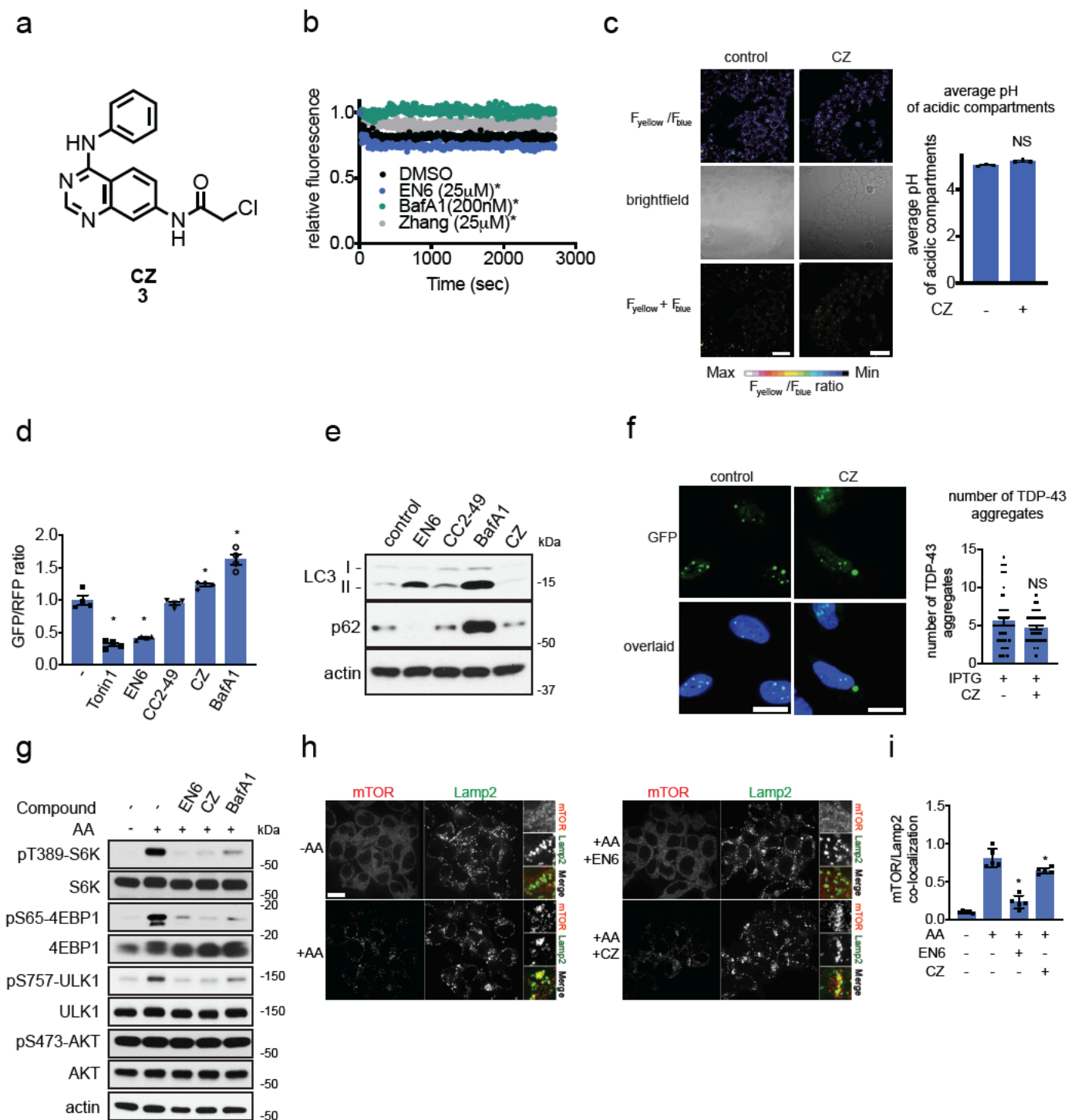
(a) Schematic of isoTOP-ABPP in which cells were pre-treated with DMSO or EN6 (50 μ M, 4 h *in situ*) prior to labeling of proteomes *in vitro* with IA-alkyne (100 μ M, 1 h), followed by appendage of isotopically light (for DMSO-treated) or heavy (for EN6-treated) TEV protease cleavable biotin-azide tags by copper-catalyzed azide-alkyne cycloaddition (CuAAC). Control and treated proteomes were subsequently combined in a 1:1 ratio, probe-labeled proteins were avidin-enriched, digested with trypsin, and probe-modified tryptic peptides were eluted by TEV protease, analyzed by LC-MS/MS, and light to heavy probe-modified peptide ratios were quantified. **(b)** Dose-response of mTORC1 signaling inhibition with DMSO vehicle or EN6 treatment in HEK293A cells for 4 h, assessed by Western blotting. Original gel images are in **Supplementary Fig. 12b**. **(c)** Time-course of mTORC1 signaling inhibition with DMSO vehicle or 25 μ M of EN6 treatment in HEK293A cells, assessed by Western blotting. Original gel images are in **Supplementary Fig. 13a**. **(d)** AKT signaling in HEK293A cells treated with vehicle DMSO, rapamycin (0.1 μ M), Torin1 (0.25 μ M), or EN6 (25 μ M) for 4 h, assessed by Western blotting. Original gel images are in **Supplementary Fig. 13b**. **(e)** Short hairpin RNA (shRNA)-mediated ATP6V1A knockdown in Hela cells, assessed by Western blotting. Original gel images are in **Supplementary Fig. 13c**. **(f)** Re-expression of Flag-tagged knockdown-resistant wild-type ATP6V1A (WT), ATP6V1A C277S mutant (C277S), or ATP6V1A C277A mutant (C277A) protein in shATP6V1A cells, assessed by Western blotting. Original gel images are in **Supplementary Fig. 13d**. **(g)** Autophagy markers and mTORC1 signaling in shControl Hela cells and shATP6V1A cells with re-expression of Flag-wild-type ATP6V1A (WT), Flag-ATP6V1A C277A mutant (C277A), or Flag-ATP6V1A C277S mutant (C277S) protein treated with DMSO vehicle or EN6 (25 μ M, 4 h), assessed by Western blotting. Original gel files are in **Supplementary Fig. 14a**. **(h)** *In vitro* v-ATPase activity measurement. Organellar fraction containing lysosomes loaded with DxOG514 were isolated from shATP6V1A HEK293T cells expressing WT, C277A, or C277S ATP6V1A. DMSO or BafA1 (200 nM) along with 5 mM ATP and MgCl₂ were added at the start of the experiment and quenching of fluorescence emission over time was measured (see methods section for details). Shown are individual replicate data points for n=4 biologically independent samples/group. **(i)** Structure of cysteine non-reactive EN6 analog, CC2-49. **(j)** Autophagy marker LC3B, mTORC1 signaling, and actin loading control protein expression levels in HEK293A cells treated with DMSO vehicle, EN6 (25 μ M), or CC2-49 (25 μ M) for 4 h, assessed by Western blotting. Bar graphs on the right show quantitation of p-S6K levels (normalized to total S6K), p-ULK1 levels (normalized to total ULK1), and LC3BII levels (normalized to actin), assessed by densitometry. Original gel files are in **Supplementary Fig. 14b**. Western blot images shown in **(b, c, d, e, f, g and j)** are representative images from n=3 (for **b-d**), n=2 (for **e, f, g**), and n=3 (for **i**) biologically independent samples/group. Bar graphs in **(j)** show average \pm sem, n=3 biologically independent samples/group. Significance in **(j)** is expressed as *p=4.4x10⁻⁵, 2.9x10⁻⁴, 0.016 for EN6-treated groups for p-S6K, p-ULK1, and LC3BII levels, respectively, compared to vehicle-treated controls, by Student's unpaired two-tailed t-test.



Supplementary Figure 3. EN6 inhibits mTORC1 lysosomal localization. mTORC1 localization in HEK293T cells with vehicle DMSO or EN6 (25 μ M) for 1 h under amino acid starvation or stimulation. Shown are representative microscopy images of mTORC1 or the lysosomal marker LAMP2. Scale bar denotes 10 μ m. Bar graph on the right shows quantitation of mTORC1/LAMP2 co-localization, expressed as average \pm sem, n=4 biologically independent samples/group. Significance is expressed as *p=8.9x10⁻⁷ compared to amino acid-stimulated vehicle-treated control, as assessed by a Student's unpaired two-tailed t-test.

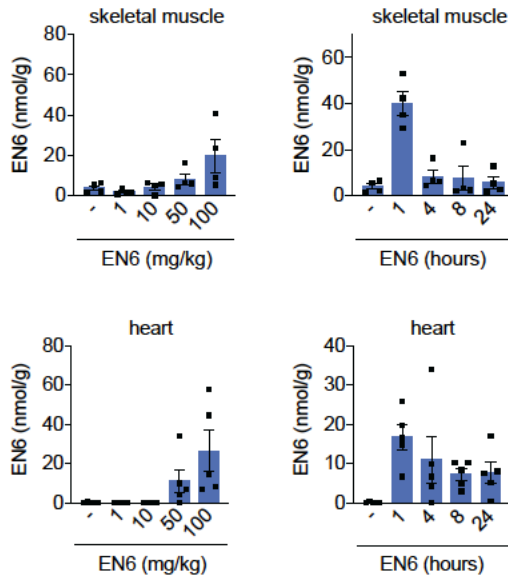
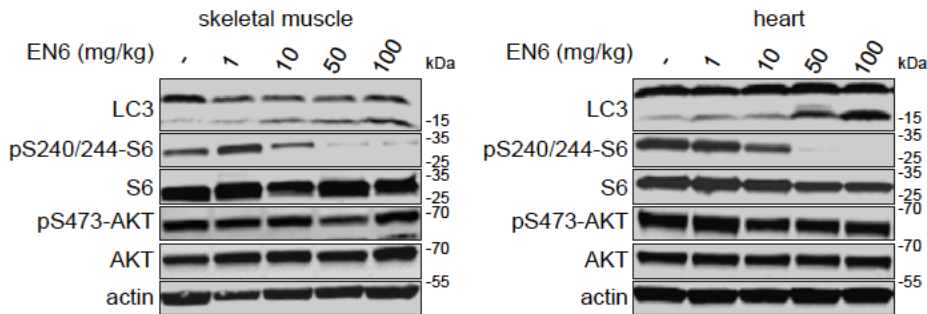


Supplementary Figure 4. Characterization of EN6 activity. (a) Localization of TFEB-GFP in HeLa cells treated with vehicle DMSO or EN6 (25 μ M, 4 h). Cells were stained with Hoechst 33342 (blue) and GFP-TFEB (green) were imaged by microscopy. Shown is the quantification of percentage of nuclear TFEB from n=6 and 7 biologically independent samples/group for vehicle-treated and EN6-treated groups, respectively, from the experiment described in Fig. 4a. (b) Protein expression levels of v-ATPase catalytic subunits in HeLa cells treated with DMSO vehicle, EN6 (25 μ M), or CC2-49 (25 μ M) for 8h, assessed by Western blotting. Shown is a representative image from n=2 biologically independent samples/group. Original gel files are in Supplementary Fig. 15a. (c) Transcript levels of genes unrelated to TFEB transcriptional programming. Gene expression of genes that are not TFEB target genes in HeLa cells treated with EN6 (25 μ M) for 0 or 8 h, assessed by qRT-PCR from n=3 biologically independent samples/group. (d) pH calibration curve for LysoSensor DND-160. HEK293A cells were stained with DND-160 (2 μ M) in DPBS at 37 $^{\circ}$ C for 5 min, washed by PBS, incubated with different pH buffer solutions in the presence of Valinomycin (10 μ M) and Nigericin (10 μ M) and imaged by LSM 880 with two-photon excitation at 730 nm. F_{yellow} and F_{blue} are emissions collected on a META detector between 400 and 490 nm, and between 514 and 649 nm, respectively. Data shown are from n=3 biologically independent samples/group. (e, f, g, h) TDP-43 aggregates in IPTG-inducible TDP-43-expressing U2OS cells assessed by measuring GFP fluorescence (e, f) or anti-GFP immunofluorescence (h). Scale bars in (f, h) denotes 20 μ m. (g, h). TDP-43 aggregate formation was induced with IPTG (1 mM) treatment for 4 h before treating cells with DMSO vehicle or EN6 (25 μ M) for 4 h. Scale bar denotes 20 μ m. Bar graphs in (f, h) show quantitation of TDP-43 aggregates, n=51 individual cells (for e, f) or n=27 individual cells (for g, h) from 3 biologically independent samples/group. Data in (c, d, f, h) expressed as average \pm sem. Statistical significance was calculated with unpaired two-tailed Student's t-tests. Significance in (a) is expressed as *p=2.8 \times 10⁻⁸ compared to vehicle-treated control groups; in (e) as *p=1.3 \times 10⁻⁷ compared to IPTG-induced vehicle-treated controls and #p=1.2 \times 10⁻⁸ compared to IPTG/EN6-treated groups; in (g) as *p=4.7 \times 10⁻¹³ compared to IPTG-induced vehicle-treated controls; in (i) as *p=9.1 \times 10⁻⁸ compared to IPTG-induced vehicle-treated controls.

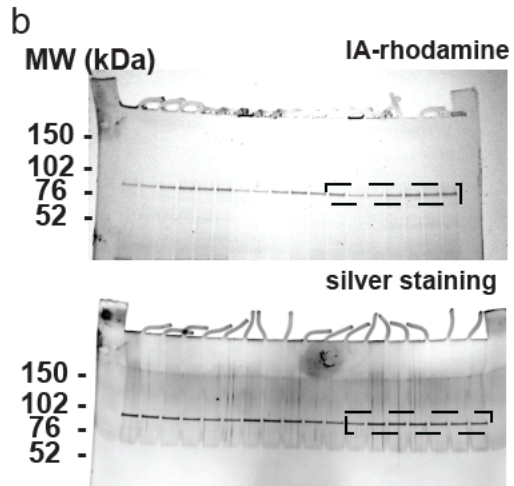
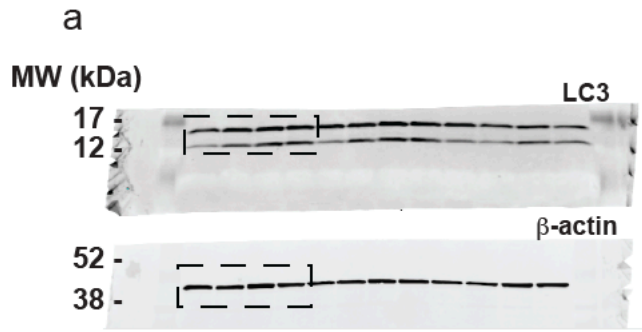


Supplementary Fig. 5. Characterization of compound CZ that targets C138 of ATP6V1A. (a) Chemical structure of CZ. (b) v-ATPase activity in response to DMSO vehicle, EN6 (25 μ M), CZ (25 μ M), or BafA1 (200 nM) was analyzed in organellar fraction containing lysosomes loaded with DxOG514 in HEK293T cells. Compounds were added with 5mM ATP and $MgCl_2$ at the start of the experiment and quenching of fluorescence emission over time was measured (see methods section for details). Shown are individual data points for $n=3$ biologically independent samples/group. (c) Confocal fluorescence imaging of pH of acidic compartments in HEK293A cells treated with vehicle DMSO or CZ (50 μ M) for 4 h, readout by LysoSensor DND-160. Microscopy images shown in (c) are representative images from $n=3$ biologically independent samples/group. Scale bar in (c) denotes 40 μ m. Bar graph on right shows quantification of lysosomal acidification. Vehicle treated control group and representative image shown are the same as the experiment reported in **Figure 4c** as these data were collected as part of the same experiment. (d) HEK293A cells

expressing a fluorescent probe GFP-LC3-RFP-LC3ΔG to measure autophagic flux, were treated with vehicle DMSO or Torin 1 (250 nM), EN6 (25 μM), CC2-49 (25 μM), CZ (25 μM), or BafA1 (200 nM) for 24 h and GFP/RFP ratios were analyzed. Data shown are from n=4 biologically independent samples/group. **(e)** LC3 and p62 levels and actin loading control levels in HEK293A cells treated with DMSO vehicle or EN6 (25 μM), CC2-49 (25 μM), BafA1 (200 nM), or CZ (25 μM) for 4 h, assessed by Western blotting. Original gel images are in **Supplementary Fig. 15b**. **(f)** Effect of CZ treatment on TDP-43 aggregate clearance. U2OS cells expressing an IPTG-inducible GFP-TDP-43 were induced with IPTG (1 mM) for 4 h before treating cells with DMSO vehicle or CZ (25 μM) for 4 h. Cells were stained with Hoechst 33342 (blue) and GFP-TDP-43 puncta (green) were imaged by confocal fluorescence microscopy. Bar graph on the right shows quantitation of TDP-43 aggregates, n=51 individual cells from 3 biologically independent samples/group. **(g)** mTORC1 and AKT signaling in HEK293A cells starved of amino acids or starved and stimulated with amino acids, in the presence of DMSO vehicle or EN6 (25 μM), CZ (25 μM), or BafA1 (200 nM) for 4 h. Original gel images are in **Supplementary Fig. 15c**. **(h)** mTORC1 localization in HEK293T cells treated with vehicle DMSO, EN6 (25 μM), or CZ (25 μM) for 1 h under amino acid starvation and stimulation. Shown are representative microscopy images of mTORC1 or the lysosomal marker LAMP2 from n=5 biologically independent samples/group. **(i)** Quantification of mTORC1 lysosomal localization in **(h)**. Data shown are from n=5 biologically independent samples/group. Blots shown in **(e, g)** are representative images of n=2 biologically independent samples/group. Data shown in **(c, d, f, and i)** as average ± sem. Statistical significance was calculated with a paired two-tailed t-test of all data for each group in **(b)** and an unpaired two-tailed Student's t-tests for **(c, d, f, i)**. Significance is expressed as *p<0.001 compared to vehicle-treated controls in **(b)**; *p=1.0x10⁻⁴, 1.9x10⁻⁴, 2.0x10⁻², 1.2x10⁻³ for Torin1, EN6, CZ, and BafA1, respectively, compared to vehicle-treated control groups in **(d)**; *p=3.0x10⁻⁵ and 0.023 for AA/EN6 and AA/CZ groups, respectively, compared to AA vehicle-treated control groups in **(i)**. NS denotes "not significant."

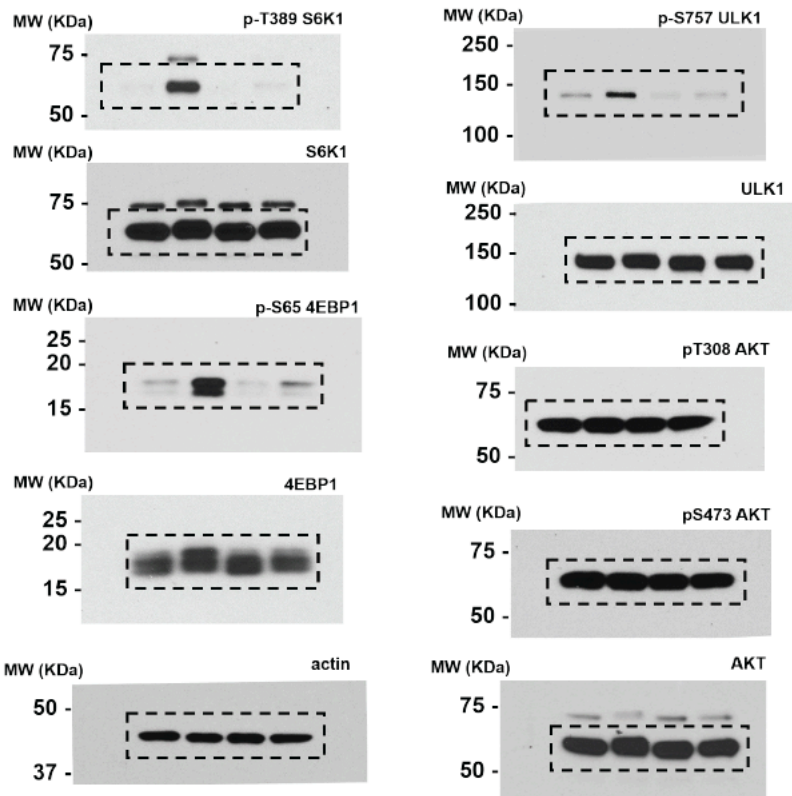
a**b**

Supplementary Figure 6. EN6 levels and its time- and dose-responsive effects in skeletal muscle and heart from mice treated by EN6 *in vivo*. (a) C57BL/6 male 6 week old mice were treated with vehicle (18:1:1 PBS:PEG40:ethanol) or EN6 through intraperitoneal (ip) injection. For time-course studies, mice were treated with EN6 (50 mg/kg). For dose-response studies, mice were treated for 4 h. EN6 levels in tissues were determined by multiple-reaction monitoring (MRM)-based LC-MS/MS. (b) Dose-responsive effects on mTORC1 signaling and LC3 levels with EN6 treatment *in vivo* in C57BL/6 male 6 week old mice. Mice were treated with vehicle (18:1:1 PBS:PEG40:ethanol) or EN6 for 4 h. Original gel files are in **Supplementary Fig. 16a-16b**. Data is expressed as average \pm sem, n=4 and n=5 biologically independent animals/group for skeletal muscle and heart, respectively, in (a) and n=4 biologically independent animals/group in (b).

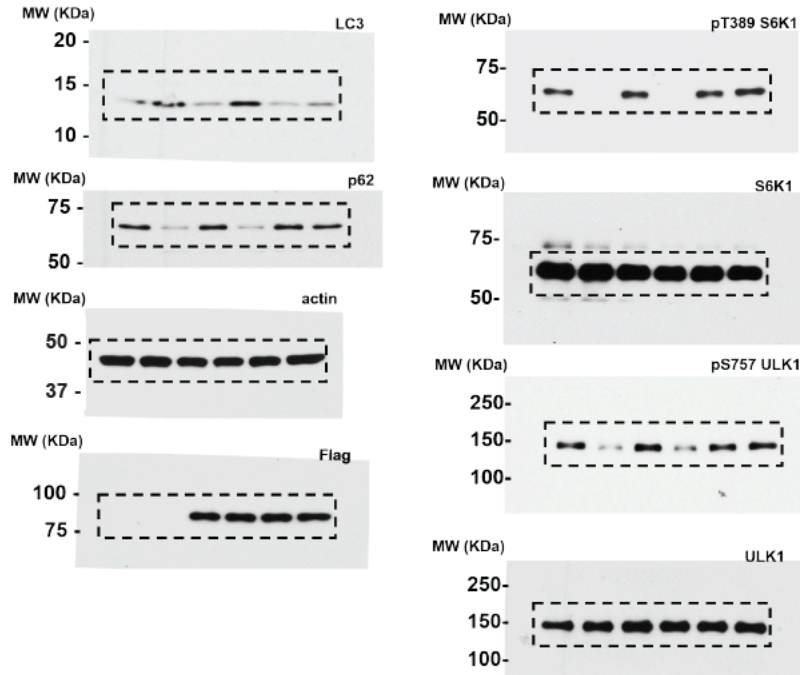


Supplementary Figure 7. Raw gel images. For all gel images, the portion of the gel cropped and used in the figures are highlighted in a dashed box. (a) Gels from Fig. 1d. (b) Gels from Fig. 2b.

a

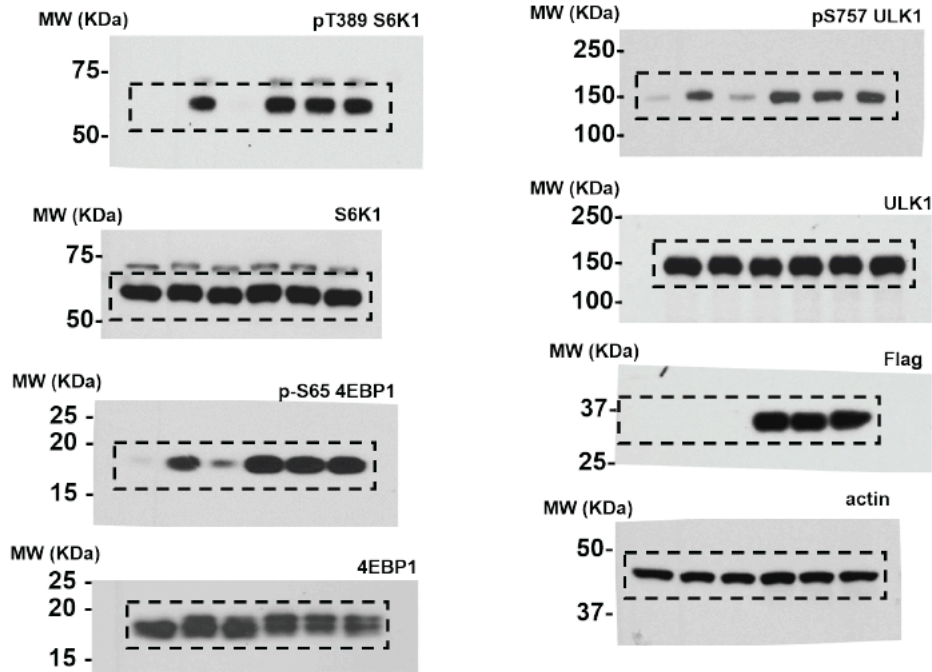


b

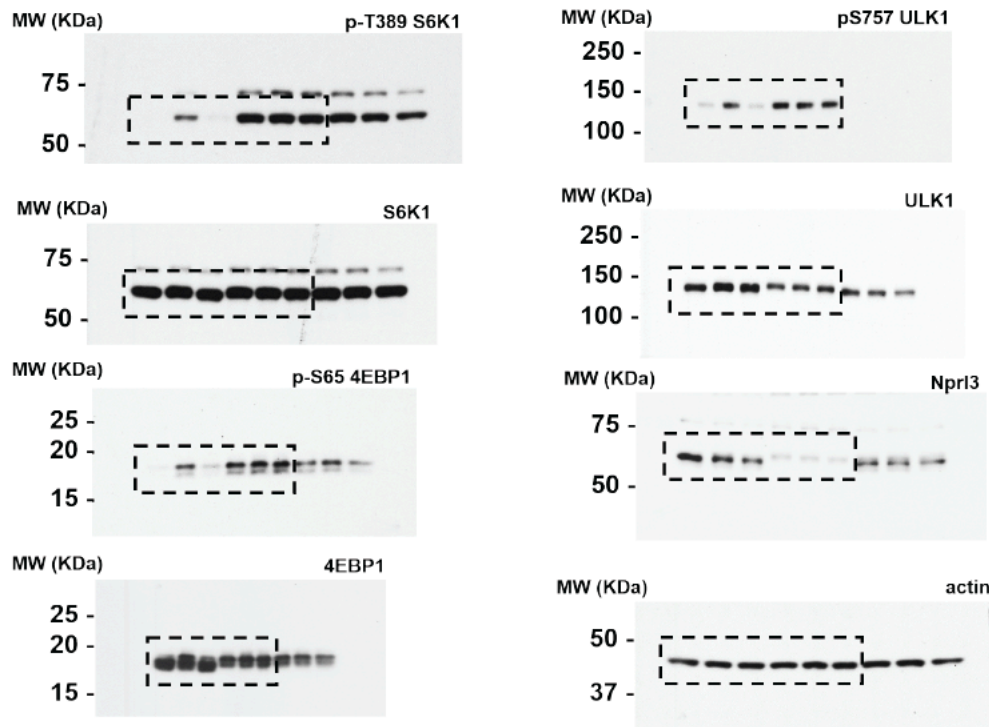


Supplementary Figure 8. Raw gel images. For all gel images, the portion of the gel cropped and used in the figures are highlighted in a dashed box. (a) Gels from Fig. 2c. (b) Gels from Fig. 2d.

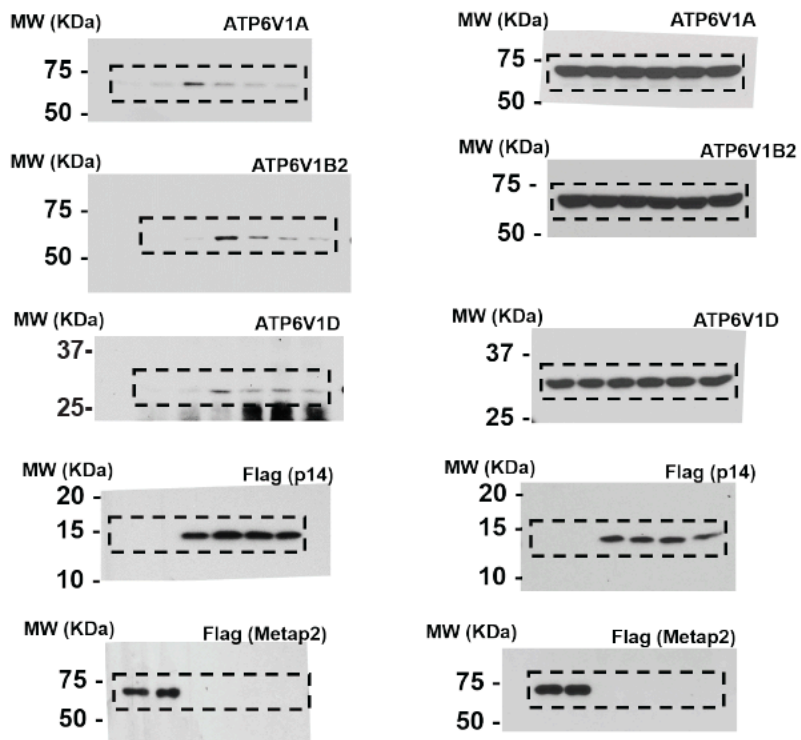
a



b

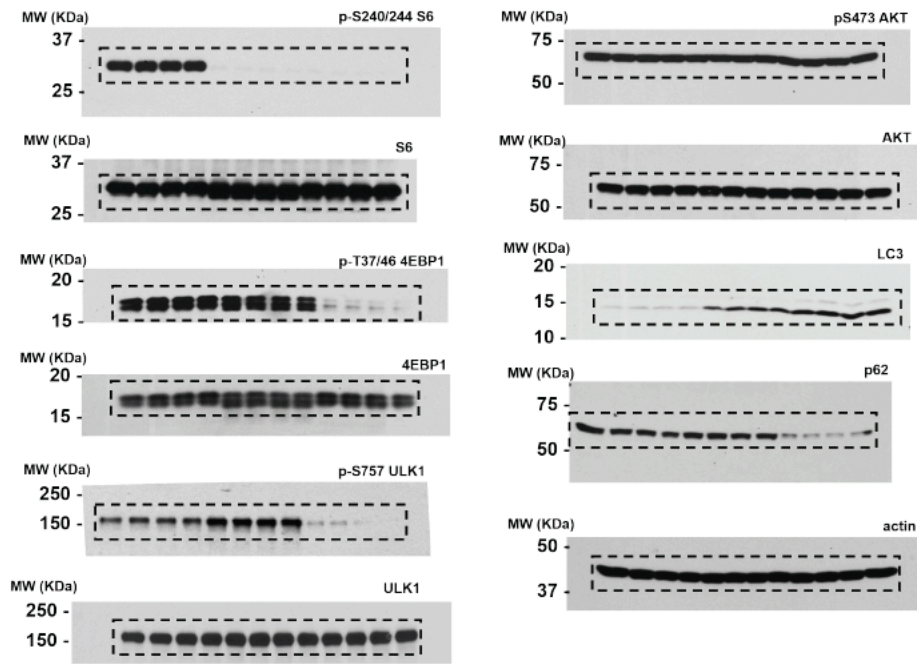


Supplementary Figure 9. Raw gel images. For all gel images, the portion of the gel cropped and used in the figures are highlighted in a dashed box. (a) Gels from Fig. 3a. (b) Gels from Fig. 3b.

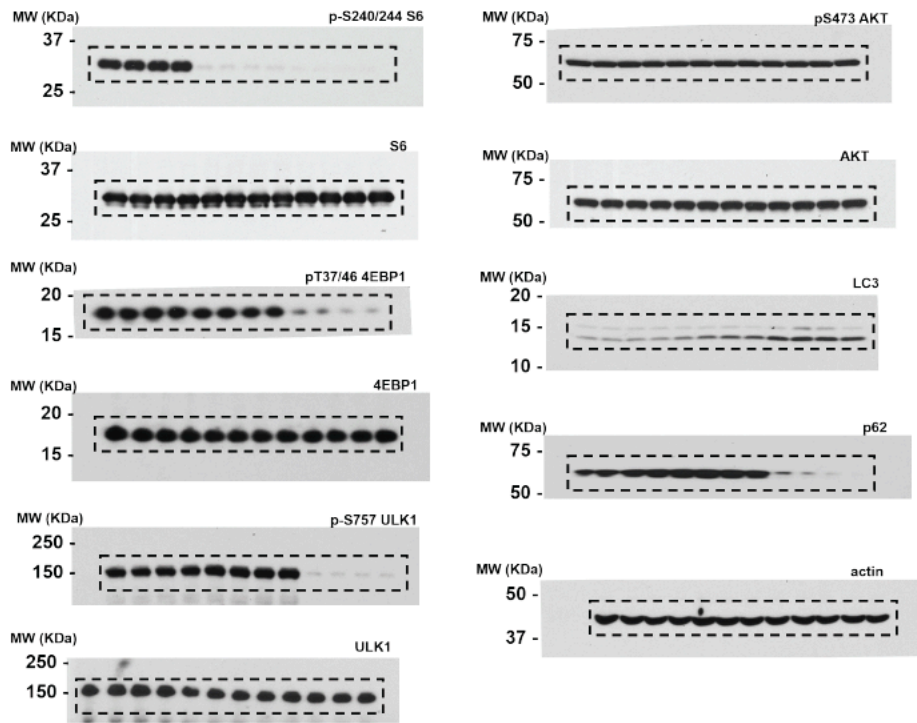


Supplementary Figure 10. Raw gel images. For all gel images, the portion of the gel cropped and used in the figures are highlighted in a dashed box. Shown is a gel from **Fig. 3e**.

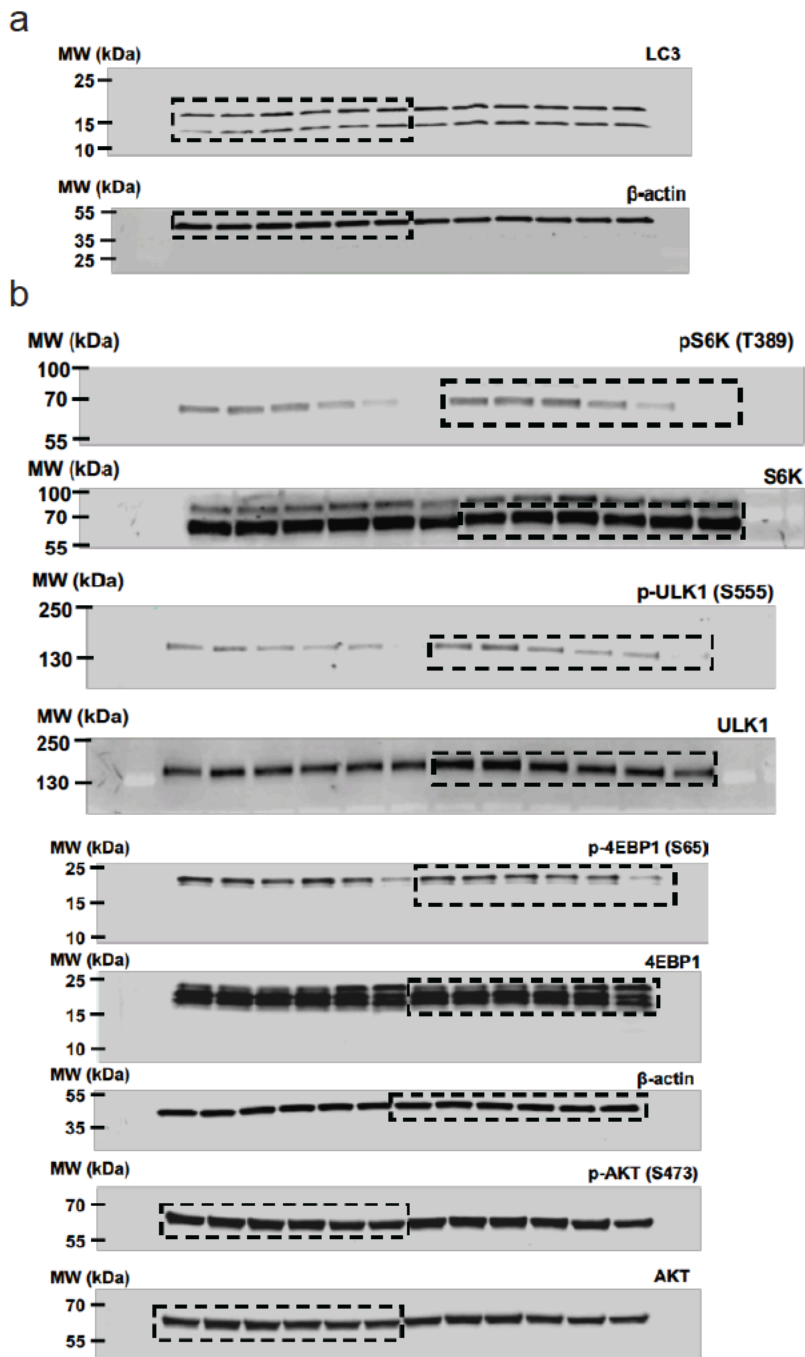
a



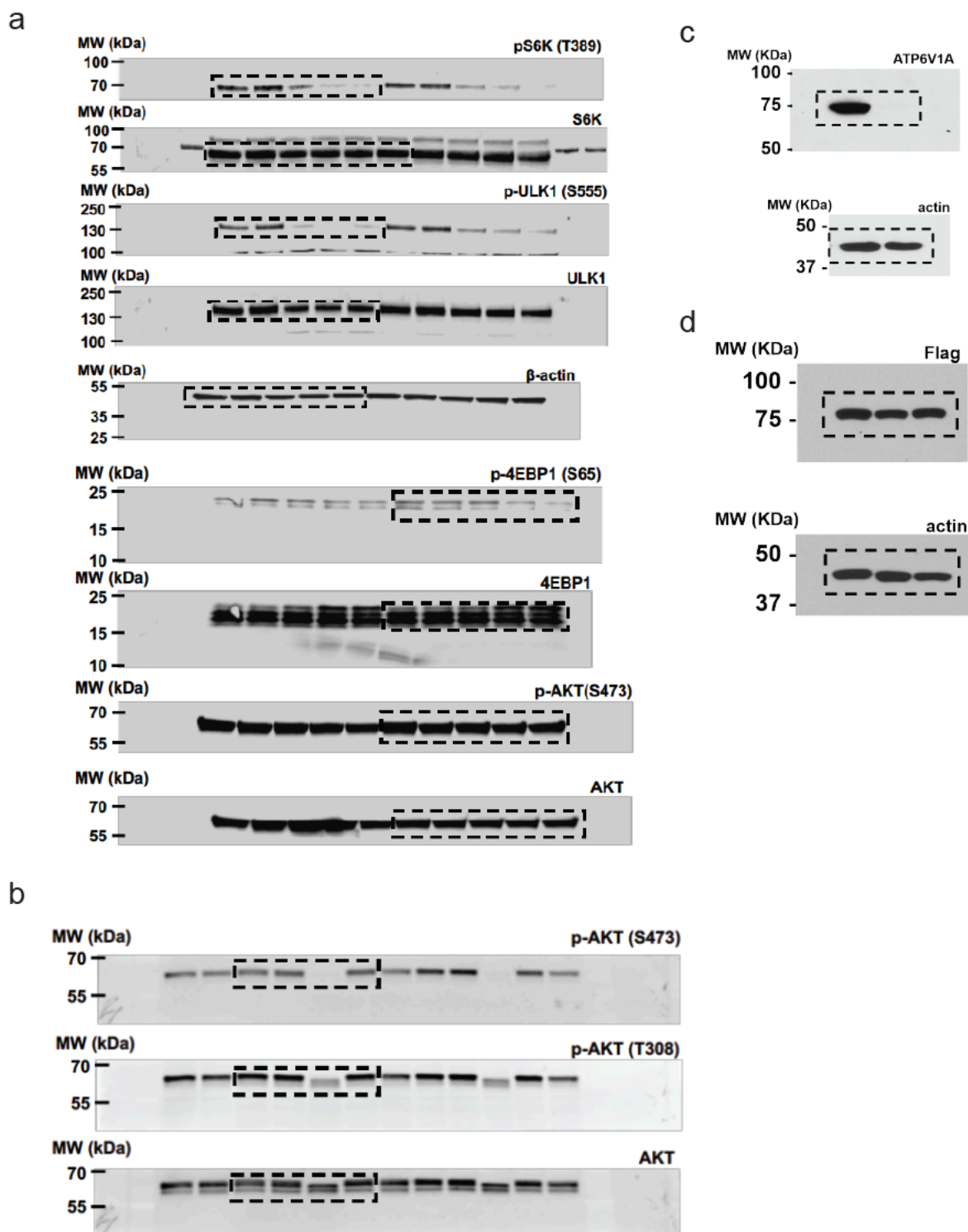
b



Supplementary Figure 11. Raw gel images. For all gel images, the portion of the gel cropped and used in the figures are highlighted in a dashed box. (a) Gels from Fig. 5a. (b) Gels from Fig. 5b.

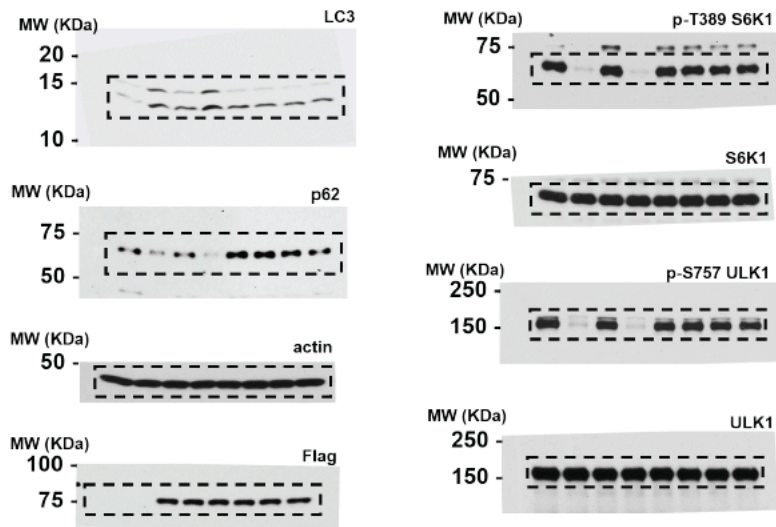


Supplementary Figure 12. Raw gel images. For all gel images, the portion of the gel cropped and used in the figures are highlighted in a dashed box. (a) Gels from **Supplementary Fig. 1a**. (b) Gels from **Supplementary Fig. 2b**.

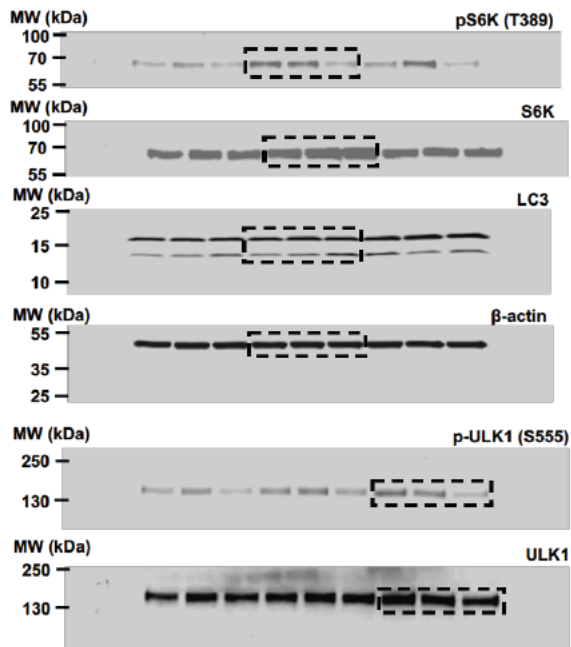


Supplementary Figure 13. Raw gel images. For all gel images, the portion of the gel cropped and used in the figures are highlighted in a dashed box. (a) Gels from **Supplementary Fig. 2c**. (b) Gels from **Supplementary Fig. 2d**. (c) Gels from **Supplementary Fig. 2e**. (d) Gels from **Supplementary Fig. 2f**.

a

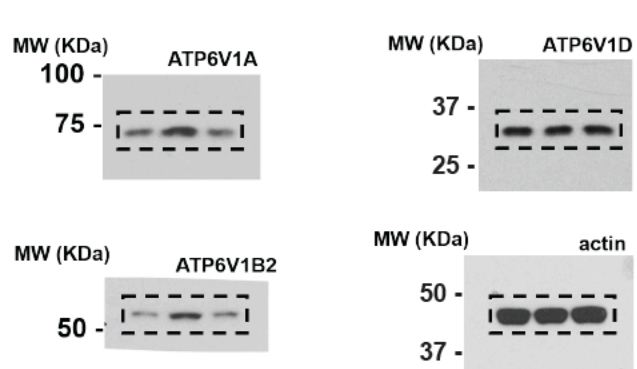


b

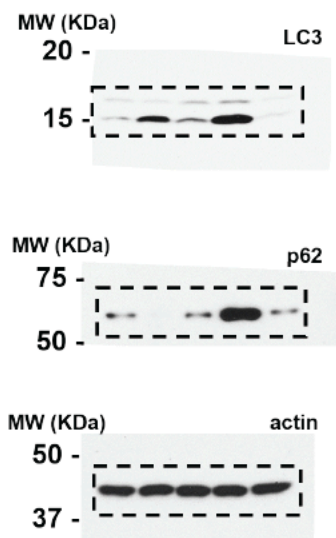


Supplementary Figure 14. Raw gel images. For all gel images, the portion of the gel cropped and used in the figures are highlighted in a dashed box. (a) Gels from **Supplementary Fig. 2h**. (b) Gels from **Supplementary Fig. 2j**.

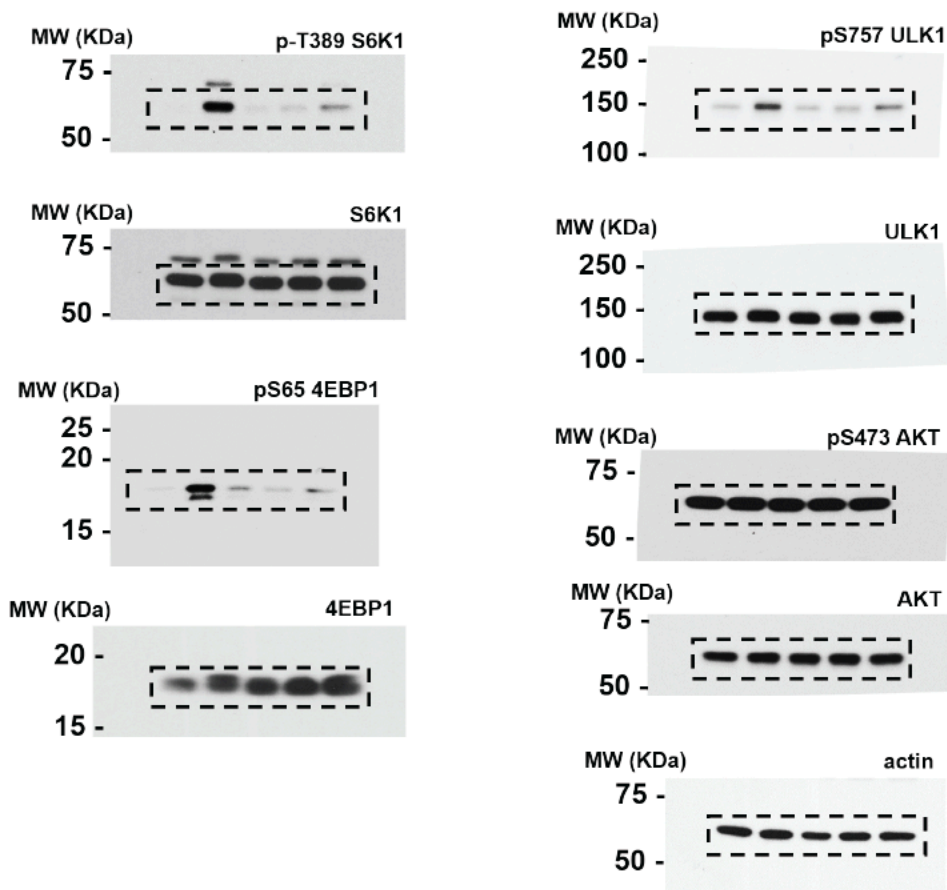
a



b

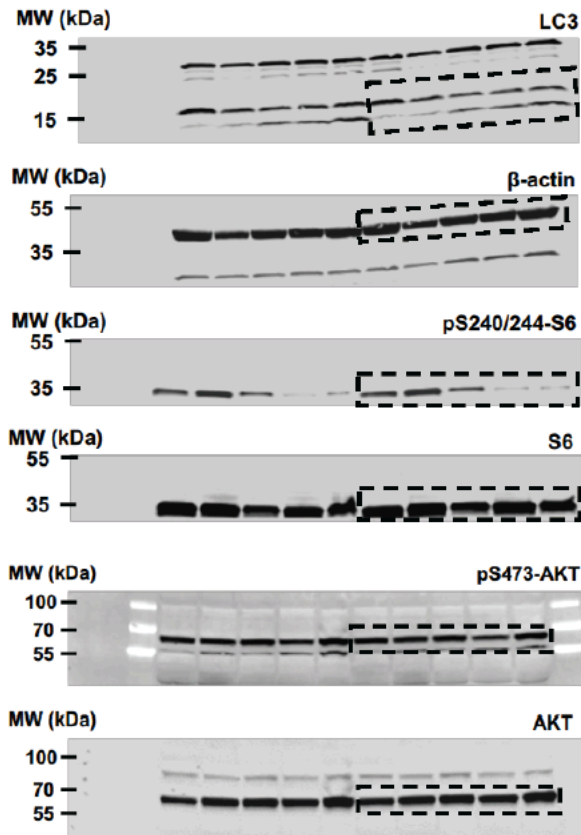


c

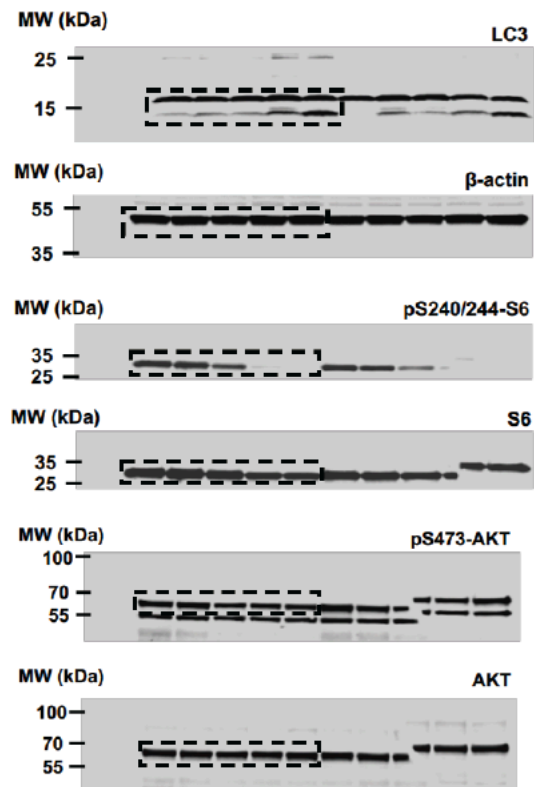


Supplementary Figure 15. Raw gel images. For all gel images, the portion of the gel cropped and used in the figures are highlighted in a dashed box. (a) Gels from **Supplementary Fig. 4b**. (b) Gels from **Supplementary Fig. 5e**. (c) Gels from **Supplementary Fig. 5g**.

a



b



Supplementary Figure 16. Raw gel images. For all gel images, the portion of the gel cropped and used in the figures are highlighted in a dashed box. **(a)** Gels from **Supplementary Fig. 6b** skeletal muscle. **(b)** Gels from **Supplementary Fig. 6b** heart.

Supplementary Datasets

Supplementary Dataset 1. Autophagy activation screening data in MEF and HEK293A cells. MEF or HEK293A cells expressing a fluorescent probe GFP-LC3-RDP-LC3ΔG to measure autophagic flux, were treated with vehicle DMSO or a covalent ligand (50 μM) for 24 h and GFP/RFP ratios were analyzed. Data shown are from n=3 biologically independent samples/group. Statistical significance was calculated with unpaired two-tailed Student's t-tests.

Supplementary Dataset 2. isoTOP-ABPP analysis of EN6 *in situ* treatment in MEF cells. MEF cells were pre-treated with DMSO or EN6 (50 μM, 4 h *in situ*) prior to labeling of proteomes *in vitro* with IA-alkyne (100 μM, 1 h), followed by appendage of isotopically light (for DMSO-treated) or heavy (for nimbolide-treated) TEV protease cleavable biotin-azide tags by copper-catalyzed azide-alkyne cycloaddition (CuAAC). Control and treated proteomes were subsequently combined in a 1:1 ratio, probe-labeled proteins were avidin-enriched, digested with trypsin, and probe-modified tryptic peptides were eluted by TEV protease, analyzed by LC-MS/MS, and light to heavy probe-modified peptide ratios were quantified. Shown are the probe-modified peptide, individual light to heavy ratios, average of ratios from each biological replicate, and average and sem of total ratios from n=3 biologically independent samples/group. Tab 1 shows all probe-modified peptides detected in this experiment. Tab 2 shows the final list of probe-modified peptides interpreted in this study. Only those probe-modified peptides that were evident across two out of three biologically independent groups were interpreted for their isotopic light to heavy ratios. Those probe-modified peptides that showed ratios >2.5 were further analyzed as potential targets of the covalently-acting small-molecule. For modified peptides with ratios >2.5, we only interpreted those peptides that were present across all three biological replicates, showed p-values <0.03, and showed good quality MS1 peak shapes across all biological replicates. Light versus heavy isotopic probe-modified peptide ratios are calculated by taking the mean of the ratios of each replicate paired light vs. heavy precursor abundance for all peptide spectral matches (PSM) associated with a peptide. Ratios that were "infinite" or >1000 due to no corresponding heavy or light signal or those ratios <0.001 were replaced with the median ratio of the remaining ratio values. The paired abundances were also used to calculate a paired sample t-test p-value in an effort to estimate constancy within paired abundances and significance in change between treatment and control. P-values were corrected using the Benjamini/Hochberg method.